

# Role of Nbs1 in the activation of the Atm kinase revealed in humanized mouse models

Simone Difilippantonio<sup>1</sup>, Arkady Celeste<sup>1</sup>, Oscar Fernandez-Capetillo<sup>1,9</sup>, Hua-Tang Chen<sup>1</sup>, Bernardo Reina San Martin<sup>2</sup>, Francois Van Laethem<sup>1</sup>, Yong-Ping Yang<sup>4</sup>, Galina V. Petukhova<sup>5</sup>, Michael Eckhaus<sup>6</sup>, Lionel Feigenbaum<sup>7</sup>, Katia Manova<sup>8</sup>, Michael Kruhlak<sup>1</sup>, R. Daniel Camerini-Otero<sup>5</sup>, Shyam Sharan<sup>4</sup>, Michel Nussenzweig<sup>2,3</sup> and André Nussenzweig<sup>1,10</sup>

Nijmegen breakage syndrome (NBS) is a chromosomal fragility disorder that shares clinical and cellular features with ataxia telangiectasia. Here we demonstrate that *Nbs1*-null B cells are defective in the activation of ataxia-telangiectasia-mutated (Atm) in response to ionizing radiation, whereas ataxia-telangiectasia- and Rad3-related (Atr)-dependent signalling and Atm activation in response to ultraviolet light, inhibitors of DNA replication, or hypotonic stress are intact. Expression of the main human *NBS* allele rescues the lethality of *Nbs1*<sup>-/-</sup> mice, but leads to immunodeficiency, cancer predisposition, a defect in meiotic progression in females and cell-cycle checkpoint defects that are associated with a partial reduction in Atm activity. The Mre11 interaction domain of Nbs1 is essential for viability, whereas the Forkhead-associated (FHA) domain is required for T-cell and oocyte development and efficient DNA damage signalling. Reconstitution of *Nbs1* knockout mice with various mutant isoforms demonstrates the biological impact of impaired Nbs1 function at the cellular and organismal level.

Mre11, Rad50 and Nbs1 (MRN) form an evolutionarily conserved protein complex that is critical for maintaining genomic stability<sup>1,2</sup>. Progress in understanding the role of MRN in mammalian cells has been hampered because loss-of-function mutations lead to early embryonic lethality in vertebrates<sup>3-6</sup>. However, partial disruption of MRN function can be compatible with viability. In humans, hypomorphic mutations in *NBS1* and *MRE11* result in NBS and ataxia-telangiectasia-like disorder (ATLD), respectively<sup>1,2</sup>. Ninety-five per cent of NBS patients carry a 5-base-pair (bp) deletion (657Δ5) in exon 6 of the *NBS1* gene, which results in the expression of two truncated proteins with relative molecular masses of 70,000 ( $M_r$  70K) and  $M_r$  26K (ref. 7). The 26K protein contains amino-terminal FHA and Brca1 carboxy-terminal (BRCT) domains, which are required for the MRN complex to accumulate into nuclear foci in response to irradiation<sup>1,2</sup>. The C-terminal species with  $M_r$  70K (Nbs1<sup>P70</sup>) is produced by an alternative initiation of translation upstream of the 5-bp deletion<sup>7</sup>, and contains Atm phosphorylation sites and the domains necessary for Mre11 interaction and Atm recruitment to double-strand breaks (DSBs)<sup>1,2,8</sup>. Although *Nbs1* domains have been characterized *in vitro*, it remains unclear which regions are critical for Nbs1 function *in vivo*.

Two viable mouse models that harbour N-terminally truncated forms of Nbs1 have been characterized<sup>9,10</sup>. In *Nbs1*<sup>ΔB/ΔB</sup> mice, replacement of

exons 4/5 in *Nbs1* by the neomycin resistance gene, and deletion of the BRCT domain, results in the expression of a truncated protein with  $M_r$  80K (ref. 10), whereas a protein with  $M_r$  75K is detectable in *Nbs1*<sup>mm</sup> mice that carry a disruption of exons 2 and 3 (ref. 9). Both mouse mutants recapitulate some of the phenotypes that are found in NBS patient cells, including cell-cycle checkpoint defects, but there are also notable phenotypic differences to human patients. For example, whereas NBS patients are prone to B-cell lymphomas, *Nbs1*<sup>mm</sup> mice develop thymic lymphomas, and *Nbs1*<sup>ΔB/ΔB</sup> mice are not susceptible to cancer. Moreover, growth retardation, female infertility, spontaneous chromosome instability and immunodeficiency, characteristics of *Nbs1*<sup>mm</sup> mice and NBS patients, were not observed in *Nbs1*<sup>ΔB/ΔB</sup> mice. The basis for these differences is unknown, but neither mouse model produces the authentic Nbs1<sup>P70</sup> mutant protein species found in NBS cells.

Nbs1 is not only a target of Atm-dependent phosphorylation, but it is also required for the dissociation of inactive Atm dimers, for facilitating Atm accessibility to protein substrates, and for optimal activation of Atm in response to irradiation<sup>11-19</sup>. In NBS and ATLD cells, the impairment in Atm activation is partial<sup>13,16,20</sup>, the phosphorylation of some substrates (for example, p53) is normal<sup>21</sup>, and the extent of the checkpoint defect is less severe than in ataxia-telangiectasia cells<sup>22</sup>.

<sup>1</sup>Experimental Immunology Branch, National Cancer Institute, National Institutes of Health, Bethesda, MD 20892, USA. <sup>2</sup>Laboratory of Molecular Immunology and <sup>3</sup>Howard Hughes Medical Institute, The Rockefeller University, New York, NY 10021, USA. <sup>4</sup>Mouse Cancer Genetics Program, National Cancer Institute at Frederick, 1050 Boyles Street, Frederick, MD 21702, USA. <sup>5</sup>Genetics and Biochemistry Branch, National Institutes of Diabetes and Digestive and Kidney Diseases, National Institutes of Health, Bethesda, MD 20892, USA. <sup>6</sup>Division of Veterinary Resources, Office of Research Services, Office of the Director, National Institutes of Health, Bethesda, MD 20892, USA. <sup>7</sup>SAIC-Frederick, National Cancer Institute-Frederick Cancer Research and Development Center, Frederick, MD 21702, USA. <sup>8</sup>Molecular Cytology Core Facility and Molecular Biology Program, Memorial Sloan-Kettering Cancer Center, New York, NY 10021, USA. <sup>9</sup>Present address: Genomic Instability Group, Molecular Oncology Program, Spanish National Cancer Center (CNIO) Madrid, 28029, Spain.

<sup>10</sup>Correspondence should be addressed to A.N. (e-mail: andre\_nussenzweig@nih.gov)

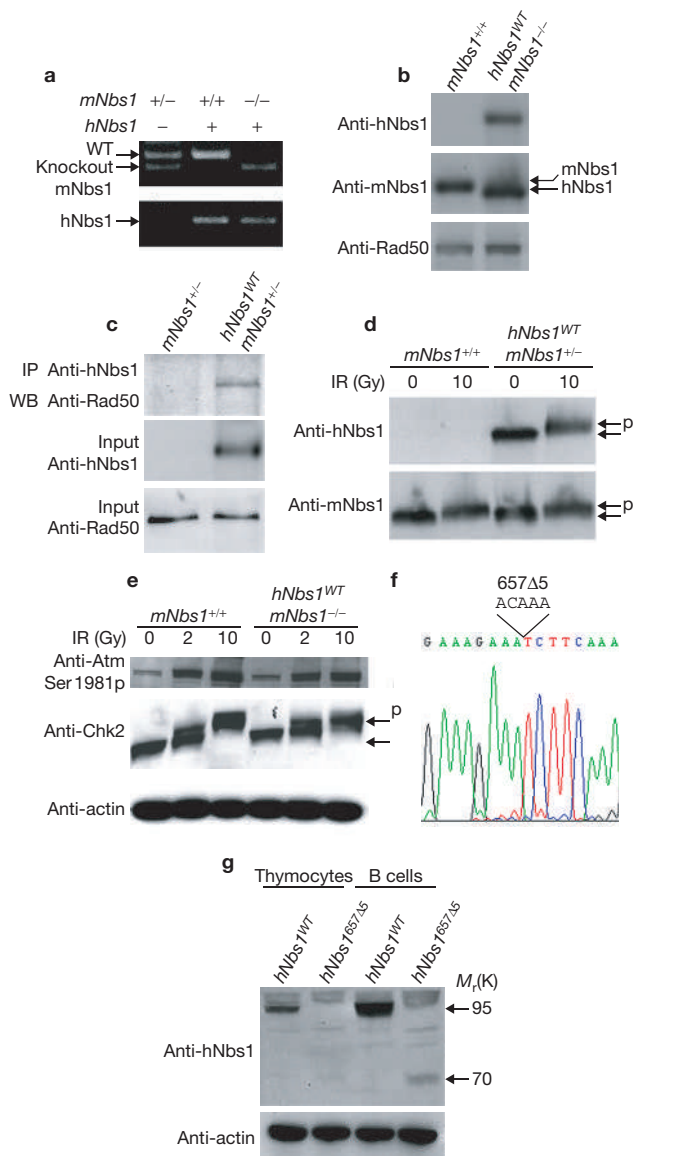


**Figure 1** Human Nbs1 functionally replaces mouse Nbs1. (a) Genotyping *mNbs1* and *hNbs1* mice by PCR. The *mNbs1* primers generate a 256-bp wild-type band and a 150-bp mutant band<sup>5</sup>, whereas the *hNbs1* primers specifically detect human *Nbs1* 255A7 BAC transgene (215-bp product). (b) hNbs1 is expressed at similar levels as mNbs1. Thymocyte extracts were blotted with anti-human Nbs1 (specific for human), anti-mNbs1 (cross-reacts with hNbs1) and anti-mRad50 antibodies. (c) hNbs1 interacts with mRad50. Thymocyte extracts from *hNbs1*<sup>WT</sup> BAC-positive and -negative transgenic mice were blotted with anti-mRad50 antibody after immunoprecipitation with an antibody recognizing hNbs1. Levels of mRad50 and hNbs1 (input) in the same extract were analysed by western blotting (WB). (d) Thymocytes were exposed to the indicated doses of ionizing radiation (IR) and cell extracts were analysed by immunoblotting with anti-hNbs1 and anti-mNbs1 30 min after treatment. hNbs1 and mNbs1 are phosphorylated after irradiation as seen by the mobility shift (p). (e) Atm and Atm substrate phosphorylation is normal in *hNbs1*<sup>WT</sup> BAC-expressing cells. Thymocytes were harvested 45 min after no treatment (0 Gy) or after irradiation (2 or 10 Gy). Phosphorylated Atm and actin was assessed by immunoblotting. Phosphorylation of Chk2 is seen by the mobility shift (p). (f) Sequence chromatogram showing the 5-bp deletion at position 657 of the *hNbs1* gene in the BAC. (g) Expression of Nbs1 in *hNbs1*<sup>WT</sup> (*hNbs1*<sup>WT</sup> *mNbs1*<sup>-/-</sup>) and *hNbs1*<sup>657Δ5</sup> (*hNbs1*<sup>657Δ5</sup> *mNbs1*<sup>-/-</sup>) thymocytes and B cells as determined by western blotting using the anti-hNbs1 antibody.

This could either reflect the incomplete penetrance of the NBS and ATLD hypomorphic alleles, or indicate that MRN-independent DNA damage sensing pathways trigger Atm activation.

Here we provide a comprehensive analysis of the domains that are critical for Nbs1 function *in vivo*. NBS is accurately modelled by *hNbs1*<sup>657Δ5</sup> *mNbs1*<sup>-/-</sup> mice (abbreviated to *hNbs1*<sup>657Δ5</sup> hereafter), which express the human 5-bp deletion hypomorphic allele. Reconstitution of *Nbs1*<sup>-/-</sup> mice with an *hNbs1* mutant lacking the Mre11 binding domain fails to rescue the lethality of the null allele. Consistent with the viability of NBS patients, *hNbs1*<sup>657Δ5</sup> mice express the C-terminal Nbs1<sup>P70</sup> protein at low levels but lack a functional N-terminal domain. Nbs1<sup>P70</sup>-containing MRN complexes retain the capacity to associate with DSBs, and to activate Atm and downstream signalling pathways. However, full complementation of *Nbs1*<sup>-/-</sup> mice requires the N-terminal FHA domain, illustrating an unexpected role for the chromatin retention of the MRN complex *in vivo*.

## RESULTS

### Human Nbs1 rescues the lethality of *Nbs1*<sup>-/-</sup> mice

We used a human bacterial artificial chromosome (BAC 255A7) containing the genomic locus that includes regulatory and coding sequences of the human *NBS1* gene<sup>23</sup> to generate *hNbs1*<sup>WT</sup> *mNbs1*<sup>-/-</sup> (abbreviated to *hNbs1*<sup>WT</sup>) mice (Fig. 1a and see Supplementary Information, Methods). To determine whether human Nbs1 can form a functional complex with Rad50 and Mre11, we performed western blot, immunoprecipitation and immunofluorescence analyses on lymphocytes derived from *hNbs1*<sup>WT</sup> mice. We found that Nbs1 and Rad50 were expressed at normal levels, that hNbs1 associated with mRad50, and that Mre11 and Nbs1 were localized in the nucleus and formed foci in *hNbs1*<sup>WT</sup> thymocytes<sup>24</sup> (Fig. 1b, c and see Supplementary Information, Fig. S1). Moreover, Atm phosphorylation at Ser 1981 as well as Atm-dependent phosphorylation of hNbs1 and Chk2 occurred normally in *hNbs1* BAC transgenic mice (Fig. 1d, e). We conclude that hNbs1 rescues the lethality of *Nbs1* knockout mice and can replace mNbs1 in a functional MRN complex.

### A humanized mouse model for Nijmegen breakage syndrome

To model NBS in mice, we used an oligonucleotide BAC recombination method<sup>25</sup> to introduce the 657Δ5 mutation into 255A7 while maintaining the integrity of the rest of the BAC. The 657Δ5 mutation was confirmed by sequencing (Fig. 1f), and the mutated BAC was subsequently used to generate transgenic mice that lacked the endogenous Nbs1. Ten founders were produced and bred to create *hNbs1*<sup>657Δ5</sup> *mNbs1*<sup>-/-</sup> mice (abbreviated to *hNbs1*<sup>657Δ5</sup>), which were born at nearly mendelian frequency. Similar to NBS patient cells, full-length Nbs1 was absent in *hNbs1*<sup>657Δ5</sup> lymphocytes, whereas Nbs1<sup>P70</sup> was barely detectable in thymocytes (data not shown) and present at low levels in activated B cells (Fig. 1g).

### Gonadal abnormalities in *hNbs1*<sup>657Δ5</sup> mice

NBS patients appear to show compromised sexual maturation, with impaired development of gonads and ovarian failure in female patients, and there is a delay in the onset of puberty in males (<http://www.emedicine.com/derm/topic725.htm>).

To determine whether Nbs1 has a role in sexual development, we examined testes and ovaries from *hNbs1*<sup>657Δ5</sup> mice. Mutant testes weighed 30–50% less than littermate controls (see Supplementary Information, Fig. S2). Histological analysis revealed that there was considerable

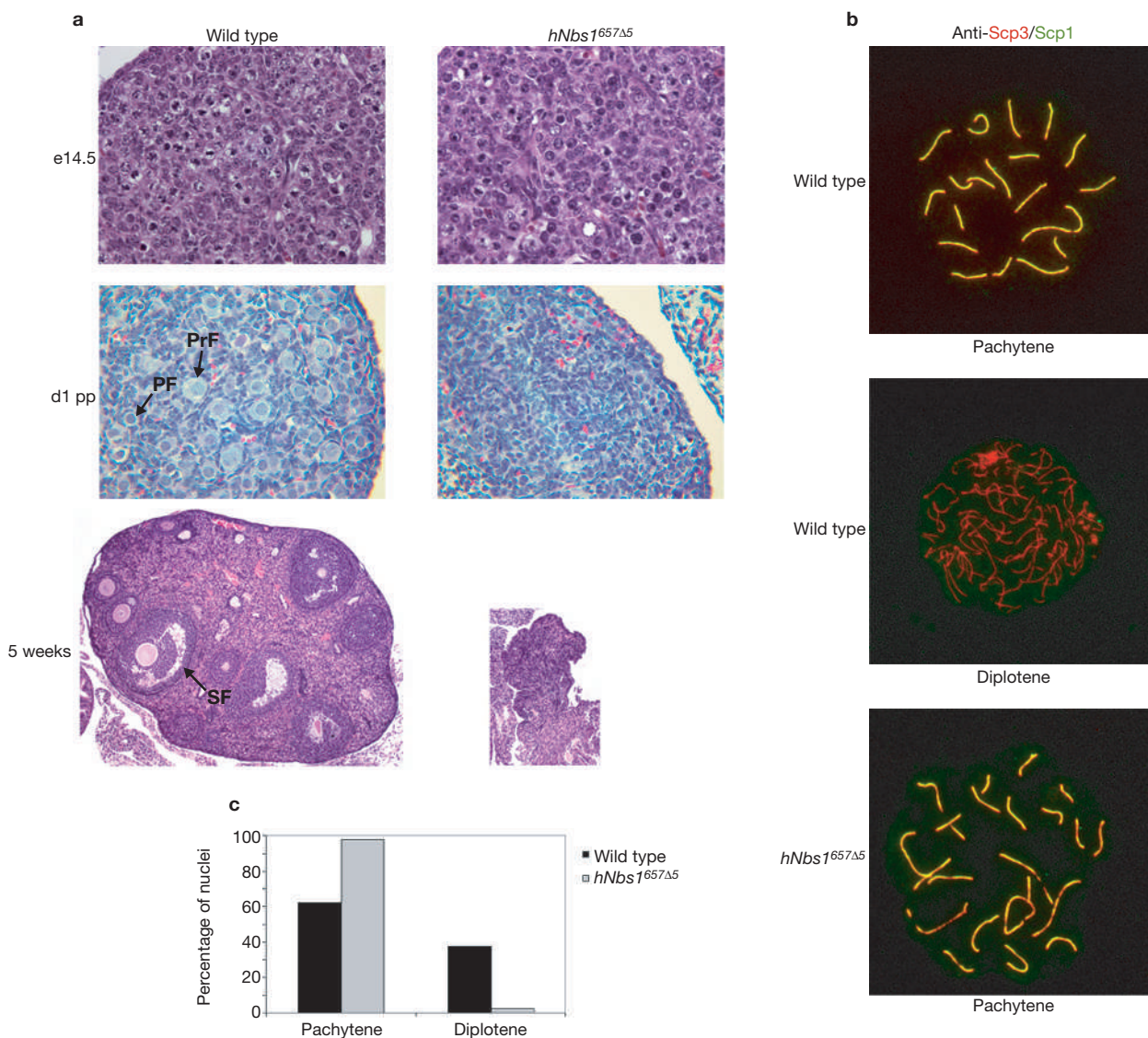


**Figure 2** Infertility in *hNbs1*<sup>657Δ5</sup> female mice. **(a)** Histological sections of fetal (upper panel; e14.5, ×60 magnification), neonatal (middle panel; day 1 post-partum (d1 pp), ×400 magnification) and 5-week-old (lower panel; ×5 magnification) ovaries from wild-type and *hNbs1*<sup>657Δ5</sup> littermates. Note the presence of primordial follicles (PF), primary follicles (PrF) and secondary follicles (SF) in wild-type mice, which are absent in the mutant ovary.

**(b)** Chromosome spreads were prepared from ovaries of newborn mice and stained with anti-Scp3 and anti-Scp1. Whereas wild-type mice show a mixture of cells in pachytene and diplotene stages, *hNbs1*<sup>657Δ5</sup> oocytes failed to progress normally to diplotene. **(c)** Quantification of cells in pachytene and diplotene in wild-type ( $n = 726$ ) and *hNbs1*<sup>657Δ5</sup> ( $n = 411$ ) newborn ovaries from littermates. The results represent data from two mice per genotype.

degeneration and an increase in the number of apoptotic cells in seminiferous tubules in *hNbs1*<sup>657Δ5</sup> mice, which was more severe in adolescent mutant males (Supplementary Information, Fig. S2). Despite a 50% reduction in sperm counts, adult *hNbs1*<sup>657Δ5</sup> males proved capable of producing offspring. The appearance of male germ cells is retarded in *hNbs1*<sup>657Δ5</sup> mice, consistent with delayed puberty in male NBS patients.

The ovaries of adult mice were small and devoid of oocytes (Fig. 2), the uterus had no evidence of oestral cycling, and *hNbs1*<sup>657Δ5</sup> females failed to breed. To determine when oocyte degeneration occurred, we examined *hNbs1*<sup>657Δ5</sup> ovaries at embryonic day 14 (e14) and 1 day after birth. No histological abnormalities were found in ovaries at e14.5, suggesting that mutant oocytes had initiated meiosis (Fig. 2a). However, newborn ovaries showed fewer germ cell cysts and primordial follicles, indicating a loss of germ cells before birth (Fig. 2a). Consistent with this, immunofluorescence

analysis of meiotic chromosome spreads revealed a severe depletion of diplotene-stage oocytes at birth. Of 726 wild-type nuclei examined, 62% were in pachytene and 38% in diplotene (Fig. 2b, c). In contrast, most (98%;  $n = 411$ ) *hNbs1*<sup>657Δ5</sup> oocytes were found in pachytene, as determined by immunostaining for the Scp3/Scp1 proteins (Fig. 2b, c). The depletion of diplotene-stage oocytes in *hNbs1*<sup>657Δ5</sup> mice provides the first direct evidence that Nbs1 is required for proper meiotic progression.

#### Impaired T-cell development in *hNbs1*<sup>657Δ5</sup> mice

NBS and ataxia telangiectasia patients have decreased numbers of T cells, and *Atm*<sup>-/-</sup> mice show abnormalities in T-cell development; these include decreased single-positive T cells, increased thymocytes expressing low levels of surface T-cell receptor (TCR), and specific translocations involving TCR loci<sup>26</sup>. We found similar defects in *hNbs1*<sup>657Δ5</sup> thymocytes

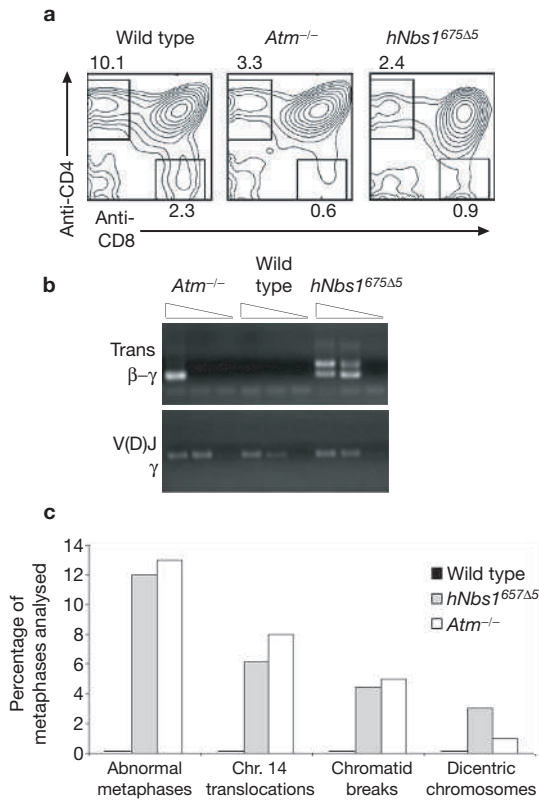
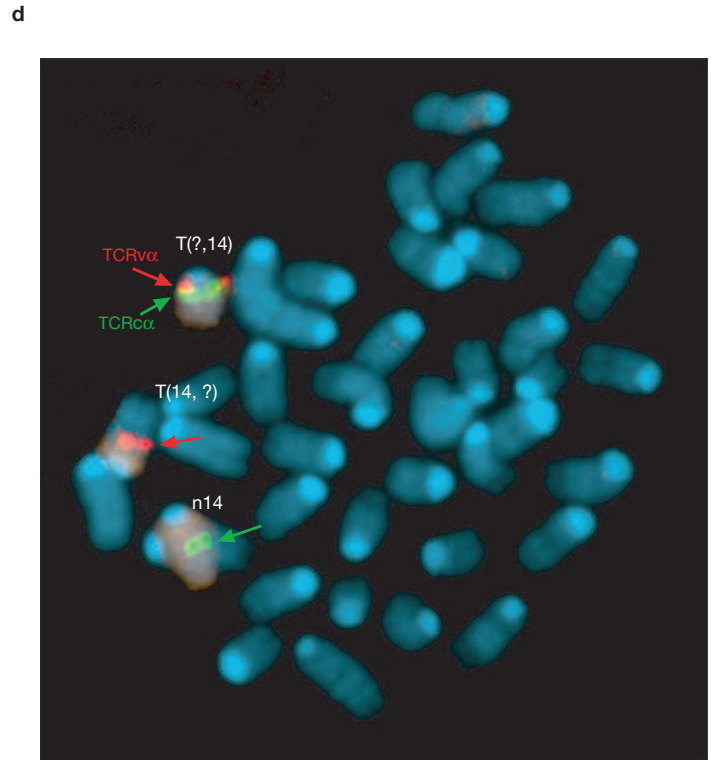


**Figure 3** Abnormal T-cell development in *hNbs1*<sup>657Δ5</sup> mice. **(a)** Flow cytometric analysis of CD4 versus CD8 surface expression in wild-type, *hNbs1*<sup>657Δ5</sup> and *Atm*<sup>-/-</sup> thymocytes. The percentage of CD4 and CD8 single-positive cells are indicated. **(b)** PCR products from normal rearrangements at the TCRγ (V(D)J γ) locus (input DNA: 100 ng, 10 ng, 1 ng) and trans-rearrangements between the *TCRβ* and *TCRγ* loci (trans β-γ) (input DNA: 500 ng, 100 ng, 10 ng) are shown. **(c)** Chromosomal abnormalities in *hNbs1*<sup>657Δ5</sup> and *Atm*<sup>-/-</sup> T cells. Chromosome aberrations were scored in 100 metaphase spreads and

including a reduction in the CD4<sup>+</sup> and CD8<sup>+</sup> compartment (Fig. 3a and see Supplementary Information, Fig. S3), a decrease in the number of single-positive cells that express high levels of CD3/TCRαβ (see Supplementary Information, Fig. S3; data not shown), and an increase in the relative number of thymocytes that expressed low levels of CD3 (see Supplementary Information, Fig. S3). Consistent with a role for Nbs1 in maintaining genomic stability in thymocytes, there was a significant increase in the levels of TCRβ-γ trans-rearrangements (Fig. 3b) and in the number of translocations, including those involving the TCRα locus (Fig. 3c, d). Altogether, 12% of *hNbs1*<sup>657Δ5</sup> and 14% of *Atm*<sup>-/-</sup> T cells showed spontaneous chromosomal aberrations, which included dicentric chromosomes, chromatid breaks, and translocations involving chromosome 14 (Fig. 3c, d). Thus, both the T-cell developmental defects and chromosomal abnormalities are very similar in *hNbs1*<sup>657Δ5</sup> and *Atm*<sup>-/-</sup> mice.

#### B-cell development and class-switch recombination in *hNbs1*<sup>657Δ5</sup> mice

Using Cre-*loxP*-mediated recombination, we generated an *Nbs1*-null mutation (*Nbs1*<sup>Δ/-</sup>) restricted to B lymphocytes<sup>27</sup>. *Nbs1*<sup>Δ/-</sup> B cells show proliferation defects and a reduction in class-switch recombination (CSR) similar to that found in *Atm*<sup>-/-</sup> B cells<sup>28,29</sup>. To determine whether there was a defect in B-cell development in *hNbs1*<sup>657Δ5</sup> mice, we analysed cells from bone marrow by flow cytometry. We found normal numbers



averaged from different animals ( $n = 2$  for *Atm*<sup>-/-</sup> and  $n = 3$  for *hNbs1*<sup>657Δ5</sup>). No abnormalities were detected in wild-type controls (*mNbs1*<sup>+/+</sup> and *hNbs1*<sup>WT</sup>). **(d)** Example of a translocation involving the *TCRα* locus in *hNbs1*<sup>657Δ5</sup> mice. Metaphase spreads were prepared from lymph node T cells and hybridized with a chromosome 14 paint (orange) and probes specific for the *TCRα* (green) and *TCRβ* (red) loci. Chromosomes were counterstained with DAPI. Normal chromosome 14 (n14) and derivative chromosomes are indicated. The *TCRβ* locus is not present in n14 due to TCR rearrangements.

of immature and mature B cells in *hNbs1*<sup>657Δ5</sup> bone marrow (data not shown). Nevertheless, as with NBS patients<sup>30,31</sup>, the levels of serum IgG1 and IgG3 isotypes were reduced in *hNbs1*<sup>657Δ5</sup> mice (Fig. 4a).

To determine whether the 657Δ5 mutation affects CSR directly, we labelled B cells from *hNbs1*<sup>657Δ5</sup> mice and from control mice with carboxy-fluorescein diacetate succinimidyl ester (CFSE), and stimulated the cells with lipopolysaccharide (LPS) alone (to induce CSR to IgG3) or with LPS+IL4 (to induce CSR to IgG1). We found that *hNbs1*<sup>657Δ5</sup> B cells proliferate normally, and that the levels of surface IgG1 and IgG3 were similar in *hNbs1*<sup>657Δ5</sup> and control mice (Fig. 4b and data not shown). Thus, in contrast to *Nbs1*<sup>Δ/-</sup> B cells<sup>27,32</sup>, *Nbs1* hypomorphic mutant B cells seem to be functionally normal.

#### Cell-cycle checkpoint defects in *hNbs1*<sup>657Δ5</sup> and *Nbs1*<sup>Δ/-</sup> B cells

Cells respond to irradiation by activating the intra-S and G2/M cell-cycle checkpoints. We compared checkpoint responses in wild-type, *Atm*<sup>-/-</sup>, *hNbs1*<sup>657Δ5</sup>, and *Nbs1*<sup>Δ/-</sup> B cells (see Supplementary Information, Fig. S4). B cells lacking Nbs1 (*Nbs1*<sup>Δ/-</sup>) showed a defective intra-S-phase and G2/M cell-cycle arrest that was similar in magnitude to that observed in *Atm*<sup>-/-</sup> cells over a dose range of 0.1 to 10 Gy (see Supplementary Information, Fig. S4). In contrast, *hNbs1*<sup>657Δ5</sup> B cells resembled their human NBS counterparts in that they failed to respond to low doses of irradiation, but induced normal checkpoints at high doses of irradiation

(see Supplementary Information, Fig. S4). We conclude that *hNbs1*<sup>657Δ5</sup> mice resemble human NBS patients in that they retain residual MRN function that is sufficient to signal the presence of DNA breaks.

### Cancer predisposition in *hNbs1*<sup>657Δ5</sup> mice

Despite the chromosomal instability and checkpoint defects, *hNbs1*<sup>657Δ5</sup> mice were not prone to early tumorigenesis, because none of the 14 *hNbs1*<sup>657Δ5</sup> mice examined over the course of 10 months died of tumours. p53 activation was normal in *hNbs1*<sup>657Δ5</sup> mice (Fig. 5). To test whether *hNbs1*<sup>657Δ5</sup> cells harbouring chromosomal abnormalities might be eliminated by p53-dependent apoptosis, we crossed *hNbs1*<sup>657Δ5</sup> mice to the *p53*<sup>-/-</sup> background. Thus far, two out of two *hNbs1*<sup>657Δ5</sup> *p53*<sup>-/-</sup> mice died before they reached 3 months of age (Fig. 4d). In contrast to *p53*<sup>-/-</sup> lymphomas<sup>33</sup>, spectral karyotyping (SKY) and fluorescence *in situ* hybridization (FISH) analysis revealed that *hNbs1*<sup>657Δ5</sup> *p53*<sup>-/-</sup> were diploid and harboured clonal non-reciprocal translocations and gene amplifications (Fig. 4c, d). FISH analysis of the B-cell lymphoma revealed that the tumour exhibited complex translocations that contained co-amplified IgHcα and c-Myc sequences. These signature cytogenetic features are shared by B-cell lymphomas that arise in *H2AX*<sup>-/-</sup> *p53*<sup>-/-</sup> mice as well as in compound non-homologous end-joining mutant/p53-deficient mice<sup>34,35</sup>. Thus, *hNbs1*<sup>657Δ5</sup> *p53*<sup>-/-</sup> mice are susceptible to both B- and T-cell lymphomas, suggesting a potential role for p53 inactivation in NBS lymphomagenesis.

### DNA damage signalling in *hNbs1*<sup>657Δ5</sup> and *Nbs1*<sup>Δ/-</sup> B cells

To examine DNA damage signalling in Nbs1-deficient cells, we exposed wild-type, *hNbs1*<sup>657Δ5</sup> and *Nbs1*<sup>Δ/-</sup> B cells to irradiation, and measured Atm activation and Atm substrate phosphorylation (Fig. 5a). Nbs1<sup>p70</sup> was present at low levels in *hNbs1*<sup>657Δ5</sup> B cells (Fig. 1g); nevertheless, Atm activation, as measured by autophosphorylation at Ser 1981 was only slightly reduced in *hNbs1*<sup>657Δ5</sup> cells (Fig. 5a). In addition, *hNbs1*<sup>657Δ5</sup> cells showed a partial reduction in the Atm-dependent phosphorylations of Smc1 at Ser 966 and Chk2 (Fig. 5a). However, the induction of p53 phosphorylation after irradiation was normal (Fig. 5a).

Although a small amount of Nbs1 could be detected in *Nbs1*<sup>Δ/-</sup> B cells (possibly due to incomplete Cre-mediated deletion)<sup>27</sup>, 5 Gy irradiation did not induce significant phosphorylation of Atm, Smc1, Chk2 or Brca1 in *Nbs1*<sup>Δ/-</sup> B cells (Fig. 5a and data not shown). Thus, loss of Nbs1 abrogates both Atm activation and Atm substrate phosphorylation in response to irradiation.

### Nbs1 is dispensable for Atr signalling and Atm activation in response to replication stress

The analysis of mitotic spreads indicates that *Nbs1*<sup>Δ/-</sup> B cells harbour a great deal of spontaneous chromosomal damage<sup>27</sup>. Despite the lack of Atm activation, stimulated *Nbs1*<sup>Δ/-</sup> B cells showed a higher percentage of cells with foci for 53BP1 (25% in wild-type (*n* = 720) versus 48% in *Nbs1* knockout cells (*n* = 501)) and MDC1 (36% (*n* = 488) in wild-type versus 56% in *Nbs1* knockout cells (*n* = 617); data not shown). Moreover, *Nbs1*<sup>Δ/-</sup> B-cell cultures exhibited elevated levels of p53 as well as p53-Ser 18p and γ-H2AX in the absence of external damage (Fig. 5a, b). This suggests that Nbs1 is required for signalling and/or repair of DSBs during normal replication.

Because Atr is thought to be the main kinase responding to replication stress, we examined the potential requirement for Nbs1 in Atr-dependent signalling. In contrast to a recent analysis of human NBS cell lines<sup>36</sup>, we found

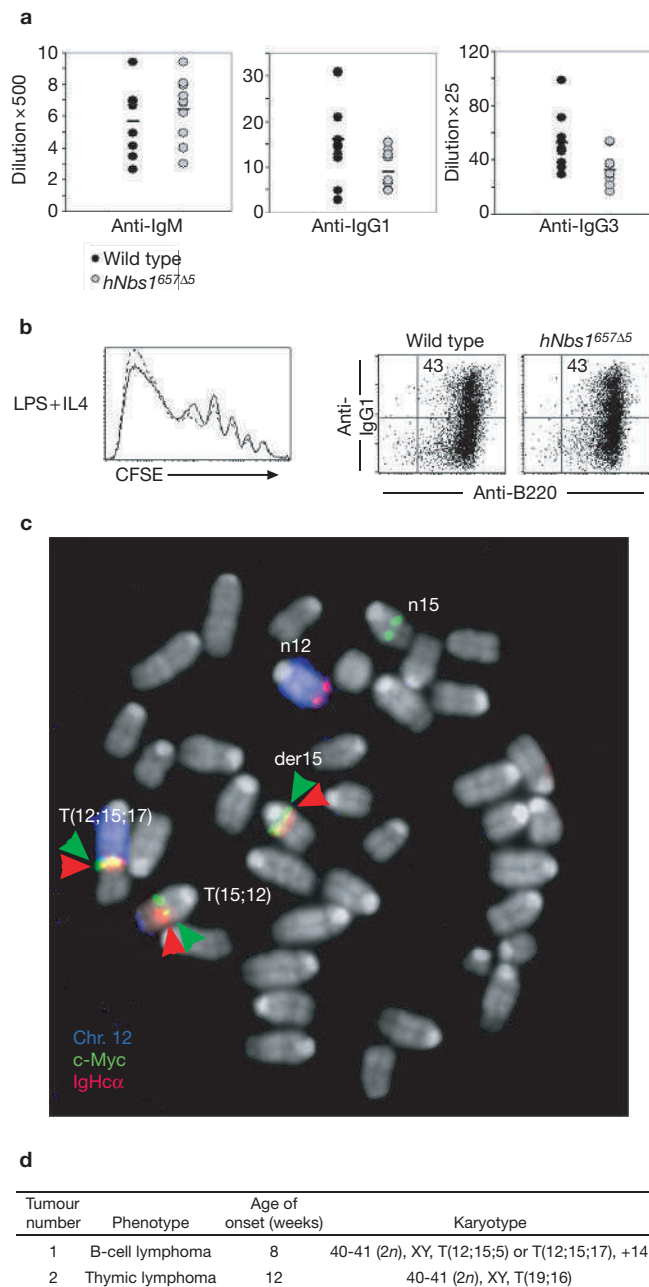


**Figure 4** Class-switch recombination and lymphoma predisposition in *hNbs1*<sup>657Δ5</sup> mice. **(a)** Sera from 6–12-week-old wild-type and *hNbs1*<sup>657Δ5</sup> littermates were collected and total IgM, IgG1 and IgG3 levels were determined by the enzyme-linked immunosorbent assay. Data are plotted as the average dilution determined in 10 mice of each genotype **(b)** Left panel: flow cytometric analysis of cell division in *hNbs1*<sup>657Δ5</sup> (dotted line) and wild-type (solid line) B cells as measured by CFSE dye dilution 96 h after stimulation with LPS + IL4. Right panel: flow cytometric analysis of surface IgG1 in the same cells. The percentage of B cells that express IgG1 are indicated. **(c, d)** Lymphomagenesis in *hNbs1*<sup>657Δ5</sup> *p53*<sup>-/-</sup> mice. **(c)** Example of a metaphase derived from a B-cell lymphoma and analysed by FISH. Chromosomes were hybridized with probes specific to IgHcα (red), c-Myc (green) and chromosome 12 (blue) and counterstained with DAPI (grey). der15, derivative 15. **(d)** Karyotype of two lymphomas from *hNbs1*<sup>657Δ5</sup> *p53*<sup>-/-</sup> mice performed by SKY.

that loss of Nbs1 did not affect the phosphorylation of Chk1 and p53 in cells treated with hydroxyurea (Fig 5b; lower panel). Thus, absence of Nbs1 does not interfere with Atr signalling.

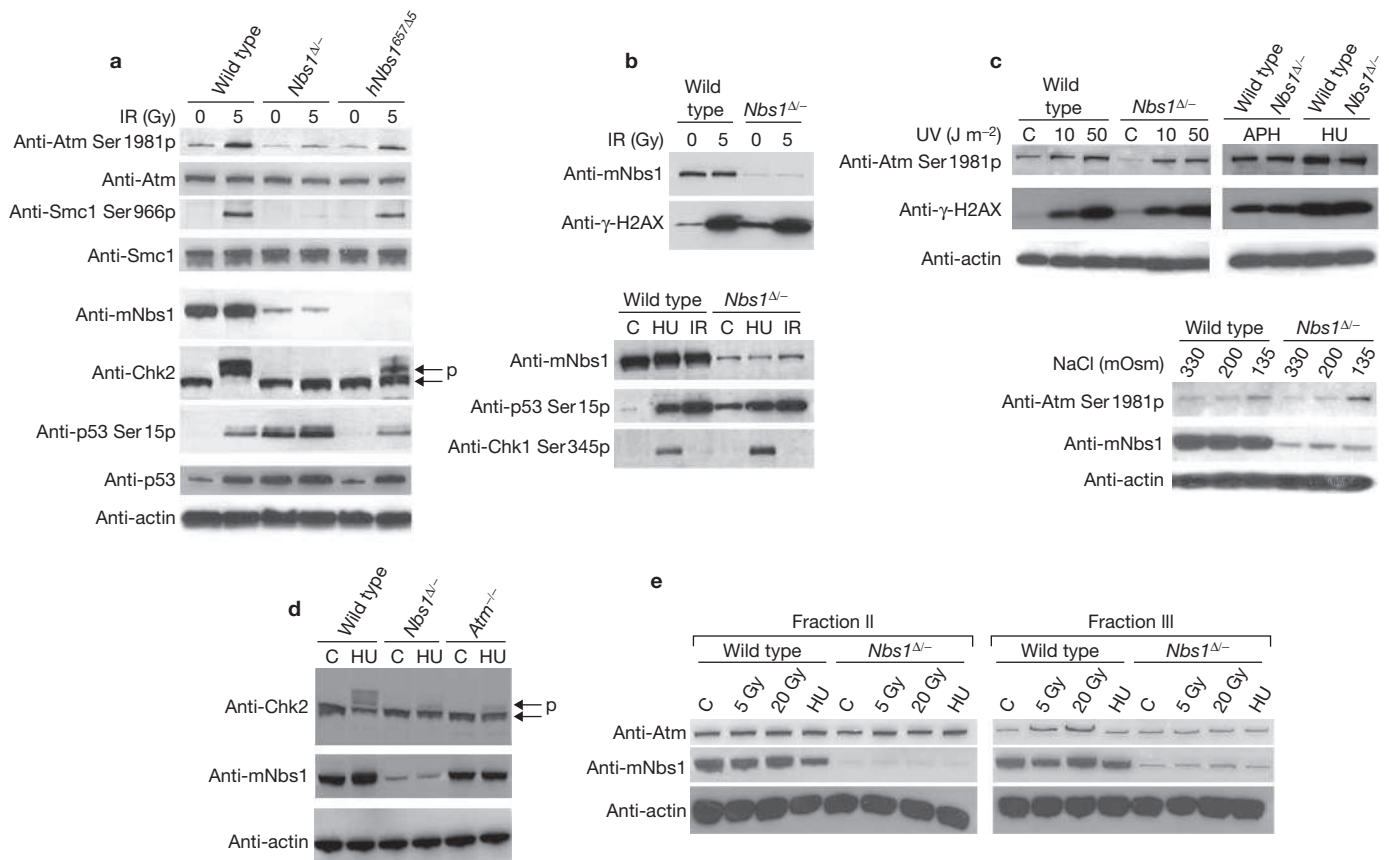


**Figure 5** Response to cellular stress in *Nbs1* knockout and hypomorphic mutant B cells. (**a–d**) Atm autoactivation and phosphorylation of substrates in wild-type (WT), *hNbs1*<sup>657Δ5</sup> and *Nbs1*<sup>Δ-/-</sup> B cells. B cells were stimulated for 48 h, and treated as indicated. (**a**) B cells were harvested 45 min after no treatment (0 Gy) or after irradiation (IR; 5 Gy). Total levels of mNbs1, Chk2, Atm, Smc1, p53 and actin, and phosphorylated Atm, Smc1 and p53 were assessed by immunoblotting. Phosphorylation of Chk2 is seen by the mobility shift (p). (**b**) Upper panel: wild-type and *Nbs1*<sup>Δ-/-</sup> B cells were harvested 45 min after no treatment (0 Gy) or after irradiation (5 Gy), and immunoblotted with anti-mNbs1 and anti-γ-H2AX antibodies. Lower panel: wild-type and *Nbs1*<sup>Δ-/-</sup> B cells were harvested 45 min after 5 Gy of irradiation, 2 h after treatment with 2 mM hydroxyurea (HU) or no treatment (C) and immunoblotted with

anti-mNbs1, and phospho-specific anti-p53 and anti-Chk1 antibodies. (**c**) Upper panel: B cells were harvested 3 h after no treatment (C), 10 J m<sup>-2</sup> UV or 50 J m<sup>-2</sup> UV, or 2 h after 5 μM aphidicolin (APH) or 2 mM hydroxyurea (HU). γ-H2AX, actin and phosphorylated Atm were assessed by western blotting. Lower panel: wild type and *Nbs1*<sup>Δ-/-</sup> were treated with 330, 200 or 135 mOsm NaCl for 1 h and mNbs1, actin and phosphorylated Atm were assessed by western blotting. (**d**) Wild-type, *Nbs1*<sup>Δ-/-</sup> and *Atm*<sup>-/-</sup> B cells were harvested 2 h after treatment with 2 mM hydroxyurea (HU) or no treatment (C) and immunoblotted with anti-mNbs1, Chk2 and actin. (**e**) Two-day B-cell cultures of wild-type and *Nbs1*<sup>Δ-/-</sup> mice were subjected to the indicated treatment, harvested and fractionated as described<sup>11</sup>. Protein (12.5 μg) from fractions II and III was loaded and immunoblotted for Atm, Nbs1 and actin.

In addition to irradiation, Atm activation is triggered by stalled DNA replication and hypotonic stress<sup>37</sup>. Consistent with this, we found that Atm-Ser 1981p was induced in wild-type B cells after treatment with ultraviolet light, hydroxyurea and aphidicolin (APH) (Fig. 5c; upper panels). Even though these treatments produced a considerable increase in DSB formation (as monitored by γ-H2AX; Fig. 5c, upper panels), autophosphorylation of Atm was not impaired in *Nbs1*<sup>Δ-/-</sup> cells (Fig. 5c, upper panels). Moreover, we found that Nbs1 was also dispensable for triggering Atm-Ser 1981p in response to hypotonic swelling (Fig. 5c, lower panel). These results indicate that Nbs1 acts upstream of Atm in response to irradiation, but is dispensable for activating Atm (and Atr) during replication and hypotonic stress.

The association of Atm with chromatin increases in response to DNA damage<sup>11</sup>. To determine whether Nbs1 affects Atm chromatin association, we extracted the soluble (fraction II) and chromatin (fraction III) Atm fractions from stimulated wild-type and *Nbs1*<sup>Δ-/-</sup> B cells. In the absence of external damage, similar amounts of Atm were resistant to detergent extraction (chromatin bound) (Fig. 5e), indicating that Nbs1

is dispensable for the association of Atm with chromatin. After irradiation treatment, we observed a substantial increase in the amount of Atm in fraction III that was dependent on the presence of Nbs1 (Fig. 5e). In contrast, hydroxyurea treatment of wild-type and *Nbs1*<sup>Δ-/-</sup> cells did not detectably alter the retention of Atm relative to unperturbed cells, indicating that Nbs1 is dispensable, both for the activation and association of Atm on chromatin in response to replication damage. Thus, the irradiation-induced activation of Atm at Ser 1981 (Fig. 5a) and increased Atm chromatin retention are dependent on Nbs1.

#### Association of Mre11 with DSBs and sites of DNA replication in *hNbs1*<sup>657Δ5</sup> cells

In wild-type B cells (Fig. 6a; left panel) or fibroblasts (see Supplementary Information, Fig. S4), most of the Mre11 is in the nucleus, whereas only 50% of the cellular Mre11 pool is present in the nucleus of NBS lymphoblastoid cell lines (LCLs)<sup>7</sup> and in *hNbs1*<sup>657Δ5</sup> B-cell nuclei (Fig. 6a; right panel). In striking contrast, Mre11 was localized exclusively to the cytoplasm in the *Nbs1* knockout cells (Fig. 6a; middle panel). Thus, Nbs1

is required to transport (or retain) Mre11 in the nucleus, and this function is only partially impaired in *hNbs1*<sup>657Δ5</sup> mice.

Because Mre11 is excluded from the nucleus (Fig. 6a), and Atm is activated in *hNbs1*<sup>657Δ5</sup> cells (Fig. 5a), we asked whether the mutant MRN complex could still associate with DSBs. DSBs were induced in discrete areas of B-cell nuclei using a laser microbeam<sup>38</sup>, and the assembly of Mre11/Nbs1 and  $\gamma$ -H2AX at these sites was tracked by fluorescence microscopy. We found that Mre11 and mutant Nbs1 were rapidly recruited to DSBs in both wild-type and *hNbs1*<sup>657Δ5</sup> B cells (Fig. 6b). Finally, a phospho-specific antibody to Nbs1 Ser 343, a prominent Atm target site contained within Nbs1<sup>P70</sup>, revealed phosphorylated Nbs1 at DSBs (Fig. 6b). Consistent with this finding, immunoprecipitation experiments have revealed that Nbs1<sup>P70</sup> is phosphorylated in response to irradiation in NBS LCLs<sup>39</sup>. In contrast, Mre11 was not recruited to the  $\gamma$ -H2AX-positive tracks in *Nbs1*<sup>Δ/-</sup> B cells (Fig. 6b). Thus, although the N-terminal FHA/BRCT domain is essential for MRN foci formation, it is not required for the initial recruitment of Mre11 or Nbs1 to DSBs.

Nbs1<sup>P70</sup> interacts with Mre11 (ref. 7) but is expressed at low levels in *hNbs1*<sup>657Δ5</sup> mice (Fig. 1g), and so the reduced nuclear pool of Mre11 may not efficiently accumulate at DSBs. Therefore, we quantified the association of Mre11 to laser damage tracks in wild-type and *hNbs1*<sup>657Δ5</sup> MEFs. Whereas both wild-type and *hNbs1*<sup>657Δ5</sup> MEFs exhibited similar levels of  $\gamma$ -H2AX induction in the laser tracks, we consistently observed less accumulation of Mre11 to DNA damage areas in *hNbs1*<sup>657Δ5</sup> cells (Fig. 7a; data not shown). Thus, the accumulation of Mre11 to DSBs is less efficient in *hNbs1*<sup>657Δ5</sup> cells.

MRN localizes with proliferating-cell nuclear antigen (PCNA) at sites of DNA replication, and it is thought to have an essential role in homologous recombination during S phase<sup>39</sup>. To determine whether Mre11 formed replication foci in *hNbs1*<sup>657Δ5</sup> cells, we used an *in situ* fractionation technique to examine the distribution of Mre11 relative to PCNA-containing DNA replication foci<sup>39</sup>. We found that Mre11 colocalized with PCNA in heterochromatic (DAPI-rich) regions in S-phase wild-type cells (Fig. 7b; upper panel). Whereas PCNA foci appeared similar in wild-type and *hNbs1*<sup>657Δ5</sup> B cells, the Mre11 staining in *hNbs1*<sup>657Δ5</sup> cells was consistently more dispersed (Fig. 7b; lower panel), although the focal accumulation of Mre11 at sites of replication was still detectable (Fig. 7b; lower panel). Taken together, our results indicate that the Nbs1 hypomorphic mutation is permissive (albeit less efficient) for MRN complex localization to sites of replication and DNA damage.

### Role of the Nbs1 FHA and Mre11 binding domains *in vivo*

Although we have demonstrated that the MRN complex in *hNbs1*<sup>657Δ5</sup> mice has partial activity, Nbs1<sup>P70</sup> is expressed at very low abundance (Fig. 1g) and it lacks the N-terminal FHA and BRCT domains of Nbs1. In NBS cell lines the N-terminal domain of Nbs1 regulates focus formation, chromatin association and cell survival in response to irradiation, but is dispensable for the nuclear localization of MRN, the activation of Atm, and the intra-S-phase checkpoint<sup>13,14,40–43</sup>. To determine the role of the FHA domain *in vivo*, we generated an inactivating point mutation at His 45 in hNbs1 (H45A), and then used the mutated BAC to generate transgenic *hNbs1*<sup>H45A</sup> *mNbs1*<sup>-/-</sup> mice lacking endogenous Nbs1 (abbreviated to *hNbs1*<sup>H45A</sup> mice). *hNbs1*<sup>H45A</sup> mice were viable and healthy and expressed the mutant Nbs1 protein at levels comparable to *hNbs1*<sup>WT</sup> mice (Fig. 8a). As expected, Mre11 failed to accumulate into irradiation-induced foci (IRIF) in mutant cells (Fig. 8b). Strikingly, female *hNbs1*<sup>H45A</sup>

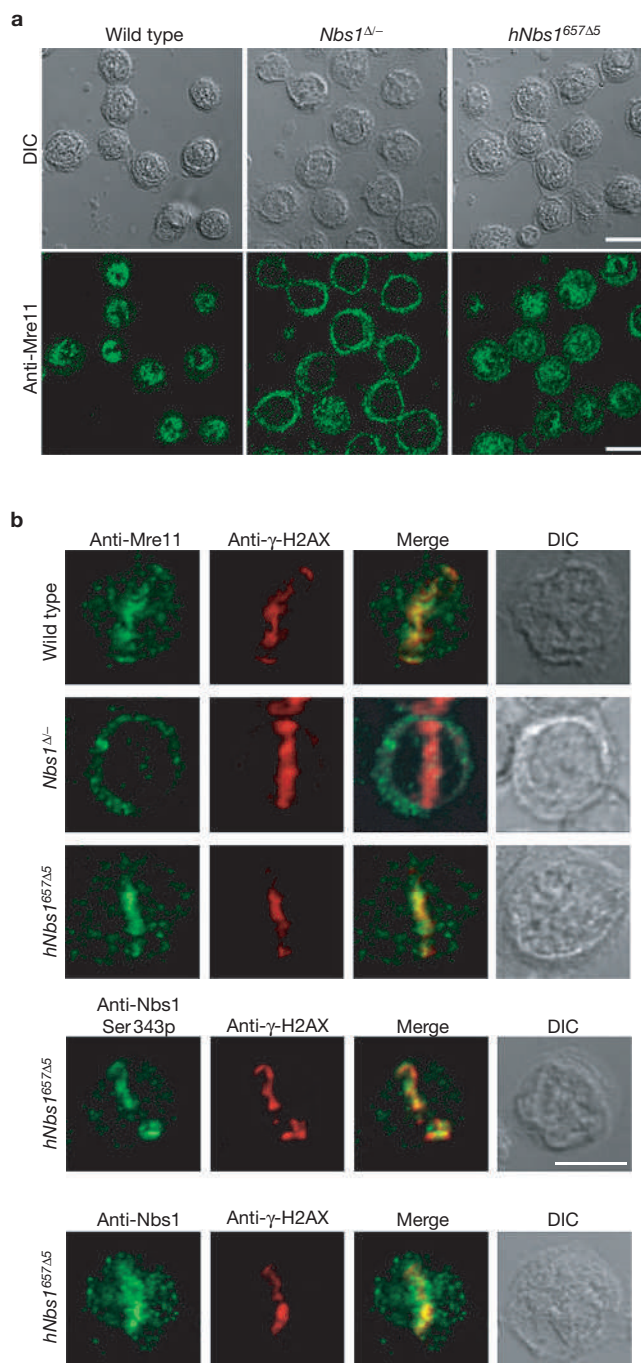


**Figure 6** Association of Mre11 with DSBs in *hNbs1*<sup>657Δ5</sup> B cells.

(a) Distribution of Mre11 in the absence of external DNA damage in wild-type (left panel), *Nbs1*<sup>Δ/-</sup> (middle panel) and *hNbs1*<sup>657Δ5</sup> (right panel) B cells. Whereas Mre11 is predominantly nuclear in wild-type cells, it is cytoplasmic in *Nbs1*<sup>Δ/-</sup> cells, and nuclear and cytoplasmic in *hNbs1*<sup>657Δ5</sup> cells. Scale bars, 10  $\mu$ m. (b) Mre11 and Nbs1 are associated with DSBs in *hNbs1*<sup>657Δ5</sup> but not in *Nbs1*<sup>Δ/-</sup> cells. Distribution of Mre11 (upper panel; green), Nbs1 Ser 343p (middle panel; green) and Nbs1 (lower panel; green) in B cells 5 min after laser scissors damage.  $\gamma$ -H2AX (red) marks sites of DSBs. Images were merged to determine colocalization. Scale bar, 8  $\mu$ m.

mice, as with *hNbs1*<sup>657Δ5</sup> mice, were sterile and their ovaries were small and lacked oocytes (Fig. 8c). Moreover, *hNbs1*<sup>H45A</sup> mice exhibited a defect in T cell development, evidenced by an increase in the relative number of cells that expressed low levels of TCR $\beta$  (similar to *hNbs1*<sup>657Δ5</sup> mice and

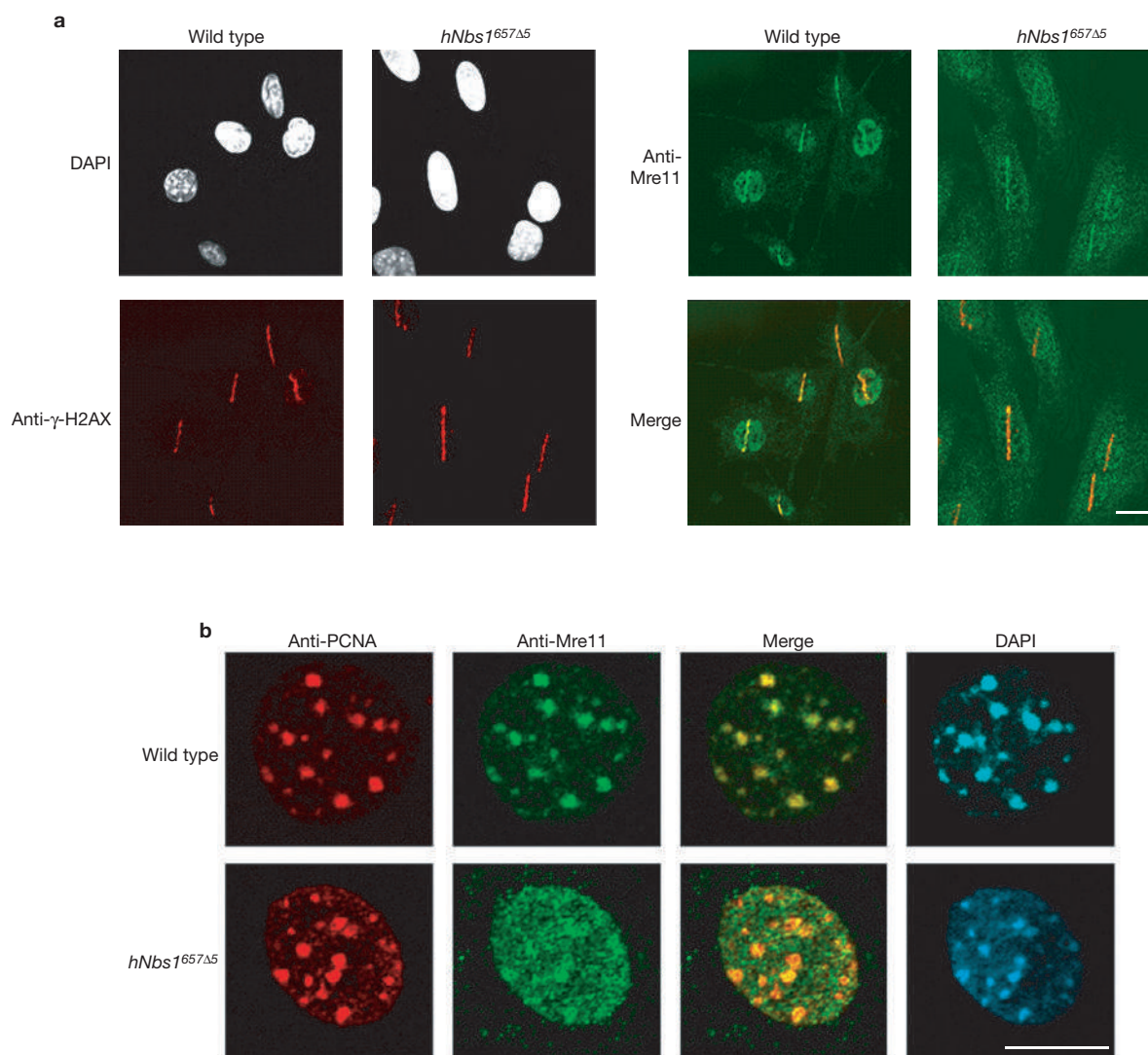


**Figure 7** Inefficient accumulation of Mre11 at DSBs and at sites of DNA replication. **(a)** Distribution of Mre11 (green) in wild-type and *hNbs1*<sup>657Δ5</sup> MEFs 5 min after damage induced by laser scissors.  $\gamma$ -H2AX (red) marks sites of DSBs. Relative to  $\gamma$ -H2AX, the accumulation of Mre11 in the damaged areas is lower in *hNbs1*<sup>657Δ5</sup> cells ( $n = 30$  for both genotypes). Settings for image acquisition were identical for both genotypes.

**(b)** PCNA (red) and Mre11 (green) staining in detergent-extracted wild-type and *hNbs1*<sup>657Δ5</sup> MEFs in the absence of DNA damage. Images were merged to determine colocalization. In wild-type cells, PCNA/Mre11 clusters are localized to heterochromatic regions coincident with intense DAPI staining (blue), whereas in *hNbs1*<sup>657Δ5</sup> MEFs the distribution of Mre11 appears more dispersed. Scale bars, 10  $\mu$ m.

less severe than *Atm*<sup>-/-</sup> mice) (Fig. 8d). Thus, inactivation of the FHA domain results in pleiotropic defects *in vivo* that resembles those found in *hNbs1*<sup>657Δ5</sup> mice.

To determine whether the Nbs1 FHA domain is critical for DNA damage signalling we examined the response of *hNbs1*<sup>H45A</sup> cells to irradiation. Spontaneous chromosomal instability in unirradiated MEFs was intermediate between *hNbs1*<sup>WT</sup> and *hNbs1*<sup>657Δ5</sup> cells. However, irradiation induced significantly more chromosomal aberrations in *hNbs1*<sup>H45A</sup> relative to *hNbs1*<sup>WT</sup> (Fig. 8e). Consistent with previous studies<sup>13,40,41</sup>, the FHA domain was not absolutely required for Atm activation or Atm-dependent phosphorylation events, because Atm-Ser 1981p and Chk2 phosphorylation was normal in *hNbs1*<sup>H45A</sup> cells irradiated at high doses (Fig. 8g and data not shown). Nevertheless, in response to low doses of irradiation (2 Gy), the phosphorylation of Chk2 was impaired (Fig. 8g). The magnitude of the signalling defect was slightly less severe than *hNbs1*<sup>657Δ5</sup> mice (Fig. 8g), and correlated with the expression level

of mutant Nbs1 (Fig. 8f). The inability of the FHA domain mutant to signal threshold levels of DNA damage may contribute to the T-cell and oocyte developmental defects in *hNbs1*<sup>H45A</sup> mice.

To determine the role of the Nbs1–Mre11 interaction *in vivo*, we placed three stop codons following amino acid 645 in Nbs1, which produces a truncation that interrupts Mre11 binding to Nbs1. The *hNbs1*<sup>tr645</sup> mutation was bred into Nbs1 heterozygous background (*hNbs1*<sup>tr645</sup> *mNbs1*<sup>+/-</sup>), which allowed us to confirm the expression of the truncated human protein (Fig. 8a). *hNbs1*<sup>tr645</sup> *mNbs1*<sup>+/-</sup> mice were healthy and fertile, but *hNbs1*<sup>tr645</sup> *mNbs1*<sup>-/-</sup> mice lacking endogenous Nbs1 were not found among 112 offspring analysed from two different *hNbs1*<sup>tr645</sup> *mNbs1*<sup>+/-</sup> founders. Thus, the Mre11-binding domain is essential for viability. On the basis of the finding that the complete sequestration of Mre11 in the cytoplasm interferes with proliferation<sup>27</sup>, we speculate that one of the essential roles of Nbs1 is to target the MRN complex to chromatin during replication and recombination.

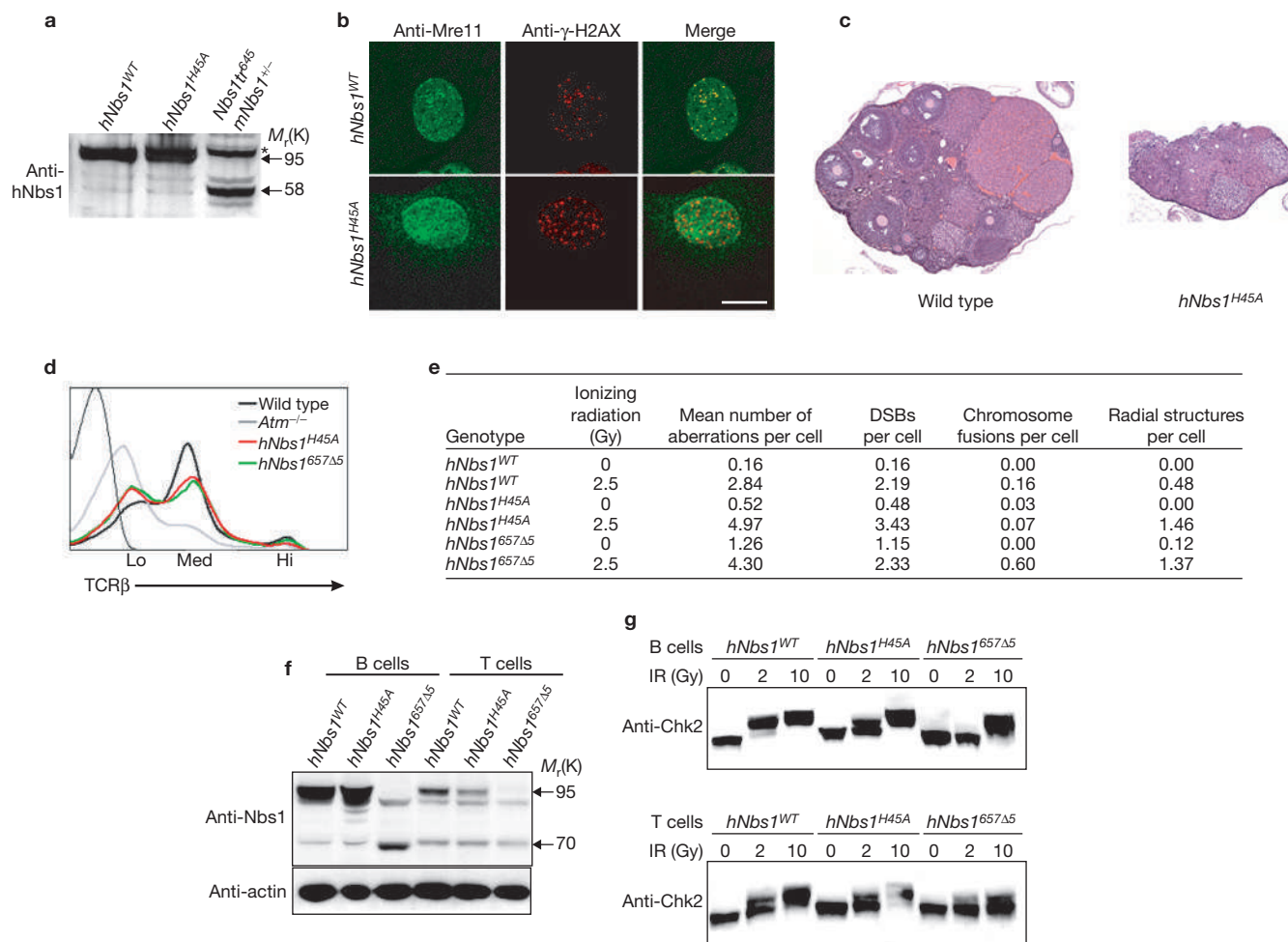


**Figure 8** Role of the Nbs1 FHA and Mre11-binding domains *in vivo*.

(a) Expression levels of wild-type, H45A and tr645 forms of hNbs1. Thymocyte extracts from *hNbs1*<sup>WT</sup>, *hNbs1*<sup>H45A</sup> and *hNbs1*<sup>tr645</sup> *mNbs1*<sup>+/+</sup> mice were blotted with anti-hNbs1 antibody. (b) Absence of irradiation induced Mre11 foci in *hNbs1*<sup>H45A</sup> MEFs. *hNbs1*<sup>WT</sup> and *hNbs1*<sup>H45A</sup> MEFs were exposed to 10 Gy of irradiation and stained 16 h later using anti-Mre11 (green) and anti-γ-H2AX (red) antibodies. Images were merged to determine colocalization. Scale bar, 10 μm. (c) Ovarian failure in *hNbs1*<sup>H45A</sup> females. Histological sections of adult (×5 magnification) ovaries from wild-type and *hNbs1*<sup>H45A</sup> littermates. (d) Defect in thymocyte development in *hNbs1*<sup>H45A</sup> mice. Histogram of TCRβ

surface expression in wild-type, *Atm*<sup>-/-</sup>, *hNbs1*<sup>657Δ5</sup> and *hNbs1*<sup>H45A</sup> thymocytes.

(e) Chromosomal abnormalities in MEFs from *hNbs1*<sup>WT</sup>, *hNbs1*<sup>H45A</sup> and *hNbs1*<sup>657Δ5</sup> mice. Metaphase spreads were prepared 16 h after exposure to 2.5 Gy irradiation or mock treatment. At least 30 metaphases per genotype per treatment were scored. DSBs reflect chromatid or chromosome breaks. (f) Nbs1 is expressed at different levels in B and T cells. Thymocyte and stimulated B-cell extracts from *hNbs1*<sup>WT</sup>, *hNbs1*<sup>H45A</sup> and *hNbs1*<sup>657Δ5</sup> mice were immunoblotted for Nbs1 and actin. (g) Chk2 phosphorylation is dependent on Nbs1 levels and the N-terminal domain. Thymocytes and stimulated B cells were harvested 45 min after no treatment (0 Gy) or after irradiation (2 or 10 Gy).

## DISCUSSION

*hNbs1*<sup>657Δ5</sup> mice provide the first model in which a transgenic human locus has been used to accurately reproduce NBS. Although some of the cellular and organismal phenotypes overlap with the previously generated models that express N-terminally truncated forms of Nbs1 (refs 9, 10), the present data also provide evidence that the incomplete penetrance of the NBS allele arises from the capacity of the mutant Nbs1 to transport Mre11 to the nucleus, to associate with sites of replication and DNA breaks, and to trigger a sub-optimal DNA damage response. Furthermore, this study provides an analysis of the domains of Nbs1 that are critical for viability, genomic stability, oogenesis and T-cell development.

Consistent with the viability of human patients, and through the finding that ectopic expression of a *NBS657Δ5* cDNA in *Nbs1*-null MEFs restores cellular proliferation<sup>44</sup>, we have found that physiological expression of the human *NBS657Δ5* mutation rescues the lethality of *Nbs1*<sup>-/-</sup> mice, which is dependent on the presence of the Mre11-binding domain

contained within Nbs1<sup>P70</sup>. *hNbs1*<sup>657Δ5</sup> mice fully recapitulate the symptoms of NBS patients because they show spontaneous chromosomal instability, immunodeficiency, cancer predisposition and gonadal abnormalities, as well as a reduction in irradiation-induced phosphorylation of *Atm* substrates and impaired cell-cycle checkpoints.

The recruitment of Mre11 to DSBs is less efficient in *hNbs1*<sup>657Δ5</sup> cells (Fig. 7a), perhaps because the low levels of the Nbs1<sup>P70</sup> truncated protein allow for only a fraction of total Mre11 in the nucleus. Moreover, the hypomorphic mutation does not completely abrogate the productive interaction of *Atm* on chromatin because Nbs1 Ser 343 and Chk2 are phosphorylated in *hNbs1*<sup>657Δ5</sup> cells. Thus, in the Nbs1 hypomorphic mutant cells, *Atm* can be activated and recruited to DSBs.

A recent study identified a region downstream of the Mre11-binding domain at the extreme C terminus of Nbs1 that serves to recruit *Atm* to sites of DNA damage<sup>8</sup>. The presence of the C-terminal domain within Nbs1<sup>P70</sup> indicates that the recruitment of both Mre11 and *Atm*

to DSBs may be decreased in proportion to the reduced levels of Nbs1. Consistent with this idea is our finding that the irradiation-induced increase in nuclear retention of Atm is abrogated in *Nbs1<sup>Δ/-</sup>* cells but is only attenuated in NBS cells<sup>11</sup>.

In contrast to the hypomorphic mutants, in *Nbs1* knockout cells Atm activation is abrogated at relatively high doses of irradiation and the magnitude of both the intra-S and G2/M checkpoint defects is similar to *Atm<sup>-/-</sup>* cells. However, Atm-Ser 1981p formation in response to replication stress is independent of Nbs1, and for either replication or irradiation damage, the presence of Nbs1 is essential for Chk2 phosphorylation, in agreement with the proposal that MRN increases the affinity of substrates to Atm<sup>12</sup>. What is the molecular basis for these disparate modes of activating Atm when damage is induced within or outside of replication forks? It is possible that a distinct set of adaptors may mediate the activation of Atm in response to irradiation versus replication stress. For example, hydroxyurea-induced activation of Atm was found to be Bloom syndrome protein (Blm)-dependent, whereas the radiomimetic bleomycin induction of Atm-Ser 1981p outside of replication forks was Blm-independent<sup>45</sup>.

Defective Atm recruitment to DSBs in NBS cells may be further compounded by the inactivation of the N-terminal FHA domain. We have found that reconstitution of *Nbs1<sup>-/-</sup>* mice with an Nbs1 isoform that disrupts the N-terminal FHA domain, while maintaining normal levels of Nbs1 expression, generates defects in T-cell and oocyte development similar to that found in *hNbs1<sup>657A5</sup>* mice. Nevertheless, genomic instability and the impairment in DNA damage signalling are less severe in *hNbs1<sup>H45A</sup>* mice. With the Nbs1 FHA domain being required for IRIF (Fig. 8b) and optimal chromatin retention of MRN complex<sup>42</sup>, and the extreme C-terminal domain being responsible for regulating the recruitment of Mre11 and Atm<sup>8</sup>, both the sustained interaction and initial recruitment of MRN/Atm-Ser 1981p with DSBs is likely to be impaired in *hNbs1<sup>657A5</sup>* mice. We conclude that both the reduced levels of Nbs1<sup>p70</sup> and dysfunction of the FHA domain contribute to the pleiotropic defects of NBS patients, whereas viability is dependent on the Mre11-binding domain. □

## METHODS

**BAC recombineering.** BAC 255A7 (Research Genetics, Invitrogen Corp., Carlsbad, CA) was mutated and mice were generated as described in the Supplementary Information Methods.

**MEFs and lymphocyte cultures.** Immortalized MEFs were generated and B lymphocytes were cultured and analysed as described<sup>27,46</sup>.

**Laser scissors and western blotting.** Generation of DSBs with laser scissors and immunofluorescence detection were performed as described<sup>38</sup>. For western blotting, cells were lysed in TNG buffer (50 mM Tris-HCl pH 7.5, 200 mM NaCl, 50 mM β-glycerolphosphate 1% Tween-20, 0.2% NP-40) containing protease inhibitors. Primary antibodies used for immunofluorescence detection and western blotting are described in the Supplementary Information Methods. Biochemical fractionation was performed as described<sup>47</sup>.

**Histology, meiotic and mitotic chromosome spreads.** Analyses of testes, ovaries and lymphocytes were performed as described in the Supplementary Information Methods.

**BIND identifiers.** One BIND identifier (www.bind.ca) is associated with this manuscript: 296546.

Note: Supplementary Information is available on the Nature Cell Biology website.

## ACKNOWLEDGEMENTS

We thank J. Petrini, S. Ganesan and A. Lee for generously providing antibodies, R. Kitagawa for experimental protocols, A. Hohenstein and N. Puri for assistance with western blotting, L. Stapleton and T. Ried for chromosome paints, M. Kastan and Y. Shiloh for helpful suggestions, and M. Difilippantonio and M. Pellegrini for comments on the manuscript. This work was supported in part by grants from NIH and the Leukemia Society to M.C.N. M.C.N. is an HHMI investigator.

## COMPETING FINANCIAL INTERESTS

The authors declare that they have no competing financial interests.

Received 8 April 2005; accepted 1 July 2005

Published online at <http://www.nature.com/naturecellbiology>.

- D'Amours, D. & Jackson, S. P. The Mre11 complex: at the crossroads of dna repair and checkpoint signalling. *Nature Rev. Mol. Cell Biol.* **3**, 317–327 (2002).
- Stracker, T. H., Theunissen, J. W., Morales, M. & Petrini, J. H. The Mre11 complex and the metabolism of chromosome breaks: the importance of communicating and holding things together. *DNA Repair (Amst)* **3**, 845–854 (2004).
- Xiao, Y. & Weaver, D. T. Conditional gene targeted deletion by Cre recombinase demonstrates the requirement for the double-strand break repair Mre11 protein in murine embryonic stem cells. *Nucleic Acids Res.* **25**, 2985–2991 (1997).
- Luo, G. *et al.* Disruption of mRad50 causes embryonic stem cell lethality, abnormal embryonic development, and sensitivity to ionizing radiation. *Proc. Natl Acad. Sci. USA* **96**, 7376–7381 (1999).
- Zhu, J., Petersen, S., Tessarollo, L. & Nussenzweig, A. Targeted disruption of the Nijmegen breakage syndrome gene NBS1 leads to early embryonic lethality in mice. *Curr. Biol.* **11**, 105–109 (2001).
- Dumon-Jones, V. *et al.* Nbn heterozygosity renders mice susceptible to tumor formation and ionizing radiation-induced tumorigenesis. *Cancer Res.* **63**, 7263–7269 (2003).
- Maser, R. S., Zinkel, R. & Petrini, J. H. An alternative mode of translation permits production of a variant NBS1 protein from the common Nijmegen breakage syndrome allele. *Nature Genet.* **27**, 417–421 (2001).
- Falck, J., Coates, J. & Jackson, S. P. Conserved modes of recruitment of ATM, ATR and DNA-PKcs to sites of DNA damage. *Nature* **434**, 605–611 (2005).
- Kang, J., Bronson, R. T. & Xu, Y. Targeted disruption of NBS1 reveals its roles in mouse development and DNA repair. *EMBO J.* **21**, 1447–1455 (2002).
- Williams, B. R. *et al.* A murine model of Nijmegen breakage syndrome. *Curr. Biol.* **12**, 648–653 (2002).
- Uziel, T. *et al.* Requirement of the MRN complex for ATM activation by DNA damage. *EMBO J.* **22**, 5612–56121 (2003).
- Lee, J. H. & Paull, T. T. Direct activation of the ATM protein kinase by the Mre11/Rad50/Nbs1 complex. *Science* **304**, 93–96 (2004).
- Horejsi, Z. *et al.* Distinct functional domains of Nbs1 modulate the timing and magnitude of ATM activation after low doses of ionizing radiation. *Oncogene* **23**, 3122–3127 (2004).
- Cerosaletti, K. & Concannon, P. Independent roles for nibrin and Mre11-Rad50 in the activation and function of Atm. *J. Biol. Chem.* **279**, 38813–38819 (2004).
- Carson, C. T. *et al.* The Mre11 complex is required for ATM activation and the G2/M checkpoint. *EMBO J.* **22**, 6610–6620 (2003).
- Kitagawa, R., Bakkenist, C. J., McKinnon, P. J. & Kastan, M. B. Phosphorylation of SMC1 is a critical downstream event in the ATM-NBS1-BRCA1 pathway. *Genes Dev.* **18**, 1423–1438 (2004).
- Costanzo, V., Paull, T., Gottesman, M. & Gautier, J. Mre11 assembles linear DNA fragments into DNA damage signaling complexes. *PLoS Biol.* **2**, E110 (2004).
- Buscemi, G. *et al.* Chk2 activation dependence on Nbs1 after DNA damage. *Mol. Cell Biol.* **21**, 5214–5222 (2001).
- Lee, J. H. & Paull, T. T. ATM activation by DNA double-strand breaks through the Mre11-Rad50-Nbs1 complex. *Science* **308**, 551–554 (2005).
- Mochan, T. A., Venere, M., DiTullio, R. A. Jr & Halazonetis, T. D. 53BP1 and NFB1/MDC1-Nbs1 function in parallel interacting pathways activating ataxia-telangiectasia mutated (ATM) in response to DNA damage. *Cancer Res.* **63**, 8586–8591 (2003).
- Lim, D. S. *et al.* ATM phosphorylates p95/nbs1 in an S-phase checkpoint pathway. *Nature* **404**, 613–617 (2000).
- Falck, J., Petrini, J. H., Williams, B. R., Lukas, J. & Bartek, J. The DNA damage-dependent intra-S phase checkpoint is regulated by parallel pathways. *Nature Genet.* **30**, 290–294 (2002).
- Tauchi, H. *et al.* Sequence analysis of an 800-kb genomic DNA region on chromosome 8q21 that contains the Nijmegen breakage syndrome gene, NBS1. *Genomics* **55**, 242–247 (1999).
- Chen, H. T. *et al.* Response to RAG-mediated VDJ cleavage by NBS1 and γ-H2AX. *Science* **290**, 1962–1965 (2000).
- Yang, Y. & Sharan, S. K. A simple two-step, 'hit and fix' method to generate subtle mutations in BACs using short denatured PCR fragments. *Nucleic Acids Res.* **31**, e80 (2003).
- Bassing, C. H. & Alt, F. W. The cellular response to general and programmed DNA double strand breaks. *DNA Repair (Amst)* **3**, 781–796 (2004).
- Reina-San-Martin, B., Nussenzweig, M. C., Nussenzweig, A. & Difilippantonio, S. Genomic instability, endoreduplication, and diminished Ig class-switch recombination in B cells lacking Nbs1. *Proc. Natl Acad. Sci. USA* **102**, 1590–1595 (2005).
- Reina-San-Martin, B., Chen, H. T., Nussenzweig, A. & Nussenzweig, M. C. ATM is required for recombination between immunoglobulin switch regions. *J. Exp. Med.* **200**, 1103–1110 (2004).

29. Lumsden, J. M. *et al.* Immunoglobulin class switch recombination is impaired in Atm-deficient mice. *J. Exp. Med.* **200**, 1111–1121 (2004).
30. Pan, Q. *et al.* Alternative end joining during switch recombination in patients with ataxia-telangiectasia. *Eur. J. Immunol.* **32**, 1300–1308 (2002).
31. Gregorek, H., Chrzanoska, K. H., Michalkiewicz, J., Syczewska, M. & Madalinski, K. Heterogeneity of humoral immune abnormalities in children with Nijmegen breakage syndrome: an 8-year follow-up study in a single centre. *Clin. Exp. Immunol.* **130**, 319–324 (2002).
32. Kracker, S. *et al.* Nibrin functions in Ig class-switch recombination. *Proc. Natl Acad. Sci. USA* **102**, 1584–1589 (2005).
33. Difilippantonio, M. J. *et al.* Evidence for replicative repair of DNA double-strand breaks leading to oncogenic translocation and gene amplification. *J. Exp. Med.* **196**, 469–480 (2002).
34. Celeste, A. *et al.* H2AX haploinsufficiency modifies genomic stability and tumor susceptibility. *Cell* **114**, 371–383 (2003).
35. Bassing, C. H. *et al.* Histone H2AX: a dosage-dependent suppressor of oncogenic translocations and tumors. *Cell* **114**, 359–370 (2003).
36. Stiff, T. *et al.* Nbs1 is required for ATR-dependent phosphorylation events. *EMBO J.* **24**, 199–208 (2005).
37. Bakkenist, C. J. & Kastan, M. B. DNA damage activates ATM through intermolecular autophosphorylation and dimer dissociation. *Nature* **421**, 499–506 (2003).
38. Celeste, A. *et al.* Histone H2AX phosphorylation is dispensable for the initial recognition of DNA breaks. *Nature Cell Biol.* **5**, 675–679 (2003).
39. Maser, R. S. *et al.* Mre11 complex and DNA replication: linkage to E2F and sites of DNA synthesis. *Mol. Cell Biol.* **21**, 6006–6016 (2001).
40. Lee, J. H. *et al.* Distinct functions of Nijmegen breakage syndrome in ataxia telangiectasia mutated-dependent responses to DNA damage. *Mol. Cancer Res.* **1**, 674–681 (2003).
41. Cersaletti, K. M. & Concannon, P. Nibrin forkhead-associated domain and breast cancer C-terminal domain are both required for nuclear focus formation and phosphorylation. *J. Biol. Chem.* **278**, 21944–21951 (2003).
42. Zhao, S., Renthal, W. & Lee, E. Y. Functional analysis of FHA and BRCT domains of NBS1 in chromatin association and DNA damage responses. *Nucleic Acids Res.* **30**, 4815–4822 (2002).
43. Tauchi, H. *et al.* The forkhead-associated domain of NBS1 is essential for nuclear foci formation after irradiation but not essential for hRAD50-hMRE11-NBS1 complex DNA repair activity. *J. Biol. Chem.* **276**, 12–15 (2001).
44. Demuth, I. *et al.* An inducible null mutant murine model of Nijmegen breakage syndrome proves the essential function of NBS1 in chromosomal stability and cell viability. *Hum. Mol. Genet.* **13**, 2385–2397 (2004).
45. Davalos, A. R., Kaminker, P., Hansen, R. K. & Campisi, J. ATR and ATM-dependent movement of BLM helicase during replication stress ensures optimal ATM activation and 53BP1 focus formation. *Cell Cycle* **3**, 1579–1586 (2004).
46. Celeste, A. *et al.* Genomic instability in mice lacking histone H2AX. *Science* **296**, 922–927 (2002).
47. Andegeko, Y. *et al.* Nuclear retention of ATM at sites of DNA double strand breaks. *J. Biol. Chem.* **276**, 38224–38230 (2001).

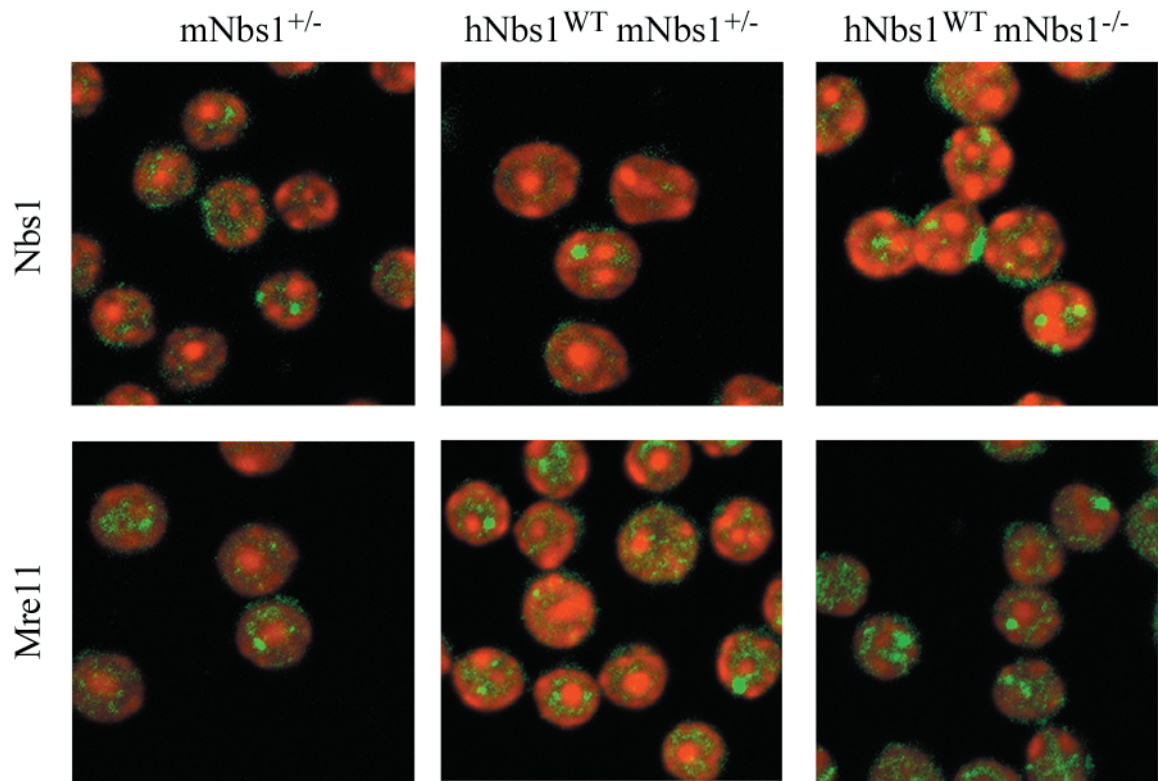


**Figure S1** Nbs1 and Mre11 foci formation in freshly isolated thymocytes from  $mNbs1^{+/-}$ ,  $hNbs1^{WT} mNbs1^{+/-}$ , and  $hNbs1^{WT} mNbs1^{-/-}$  mice.

Thymocytes were stained for Nbs1 (upper panel) or Mre11 (lower panel) and counterstained with Topro-3 (red).

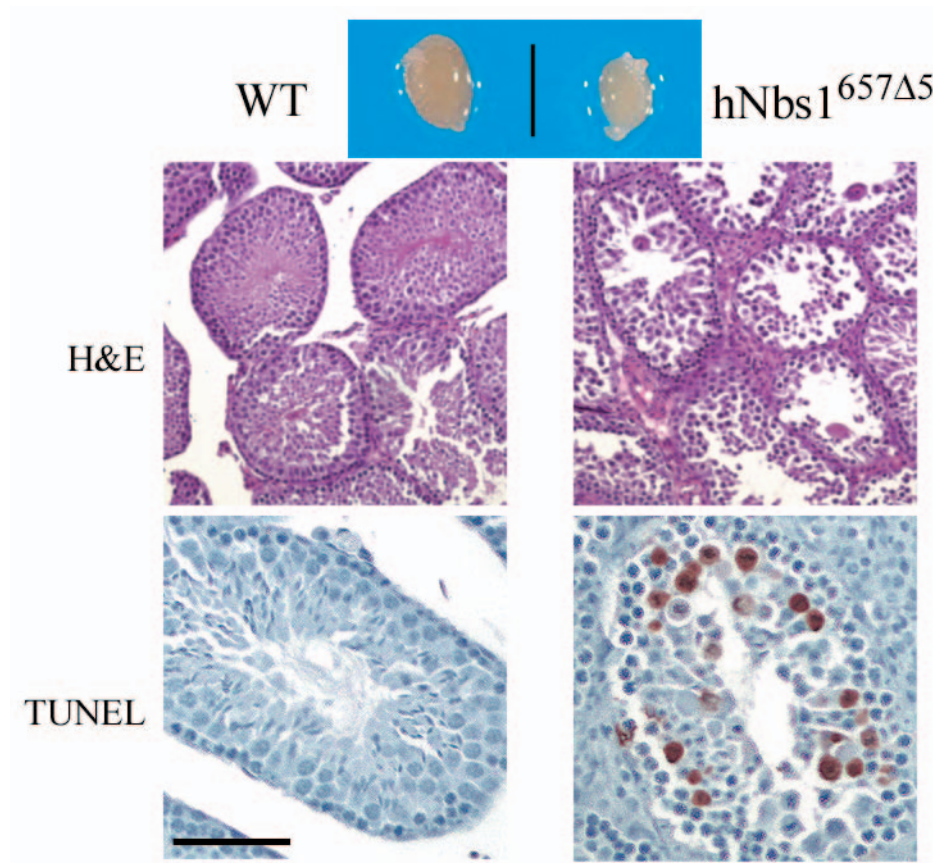


**Figure S2** Delayed germ cell development in male hNbs1<sup>657Δ5</sup> mice. (a) Photographs of testes and histological sections of seminiferous tubules of 33-day old WT and hNbs1<sup>657Δ5</sup> mice. Sections were stained with hematoxylin-eosin (upper panel), and tubules were examined for apoptotic cells by the TUNEL *in situ* assay (lower panel; scale bar represents 68 μM). hNbs1<sup>657Δ5</sup> testes are smaller and mutant tubules showed extensive apoptosis. These alterations were more severe in adolescent hNbs1<sup>657Δ5</sup>

males, and very few tubules were found to contain mature sperm in 33 day-old mice. However, sperm was eventually produced as seen in cross sections of tubules from adult (46-, 78- and 96-day old) hNbs1<sup>657Δ5</sup> mice (not shown), and confirmed by the analysis of sperm counts in epididymal tissue (hNbs1<sup>657Δ5</sup>: 10.2± 0.9 x 10<sup>6</sup> vs. WT: 21± 2.2 x 10<sup>6</sup> sperm from 46 day-old caudae epididymis).

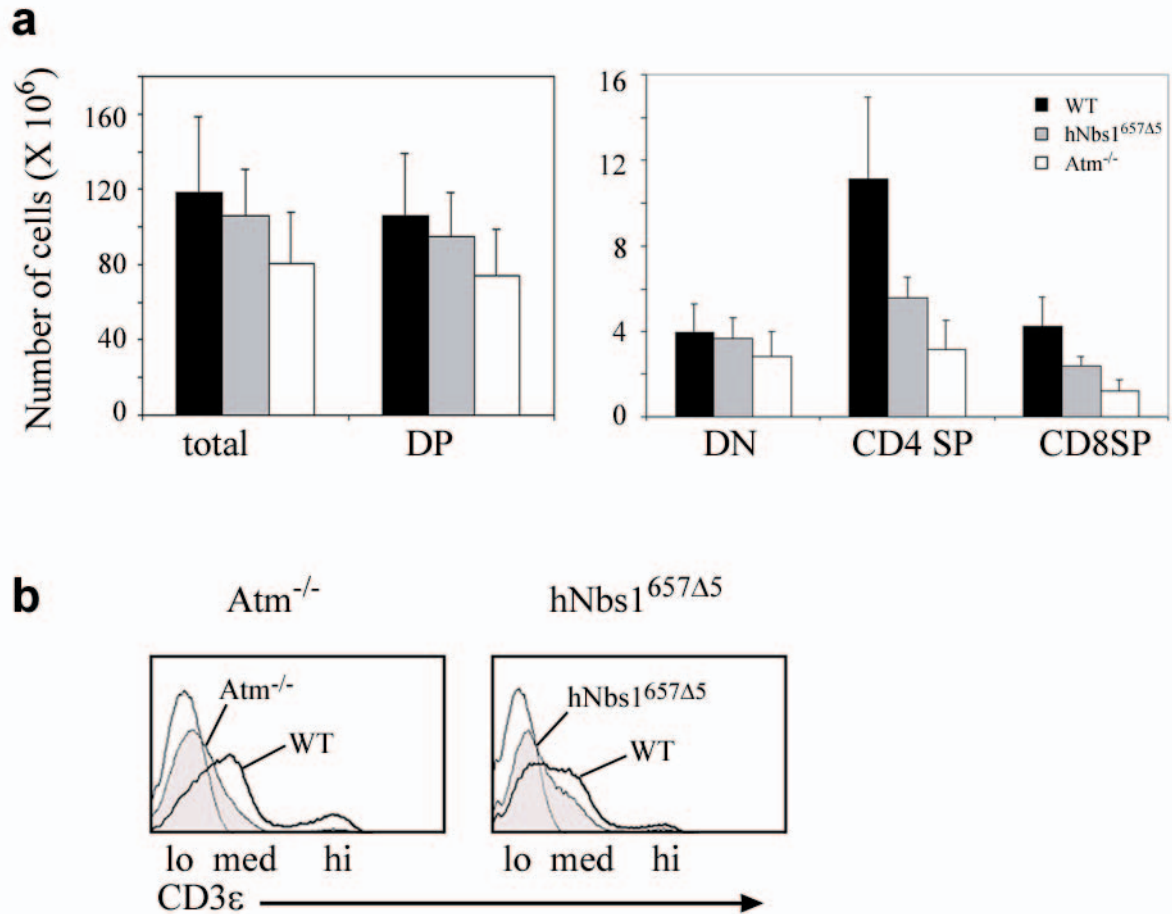


**Figure S3** Defective T cell development in hNbs1<sup>657Δ5</sup> mice. **(a)** Comparison of thymocyte subpopulations in hNbs1<sup>657Δ5</sup> (gray bars), Atm<sup>-/-</sup> (white bars) and WT (Nbs1<sup>+/+</sup>, black bars) mice (DP, CD4<sup>+</sup>8<sup>+</sup>; DN, CD4<sup>-</sup>8<sup>-</sup>; CD4<sup>+</sup>SP, CD4<sup>+</sup>8<sup>-</sup>; CD8<sup>+</sup>SP, CD4<sup>-</sup>8<sup>+</sup>) (For each genotype, at least 5 mice at 4-6

weeks of age were examined). **(b)** Histogram of CD3ε surface expression in Atm<sup>-/-</sup> vs. Atm<sup>+/+</sup> (left panel) and hNbs1<sup>657Δ5</sup> vs. Nbs1<sup>+/+</sup> (middle panel) thymocytes.

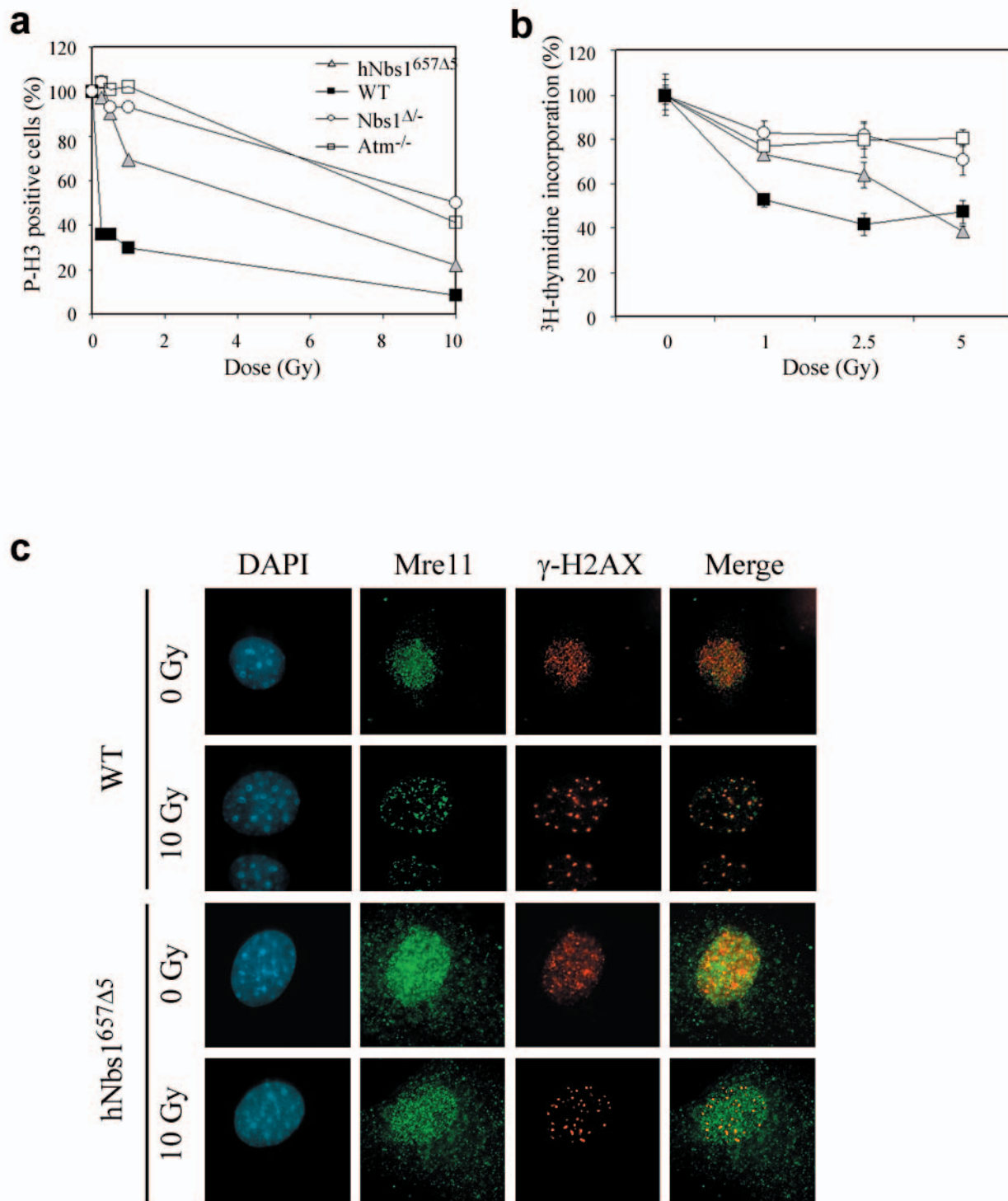


**Figure S4** Defects in IR induced checkpoints and foci formation in hNbs1<sup>657Δ5</sup> cells. (a) Comparison of the G2/M checkpoint in hNbs1<sup>657Δ5</sup> (gray triangles), WT (black squares), Nbs1<sup>Δ/-</sup> (open circles) and Atm<sup>-/-</sup> (open squares) mice. B cells were stimulated for 48 hours, irradiated with the indicated dose, and the mitotic cells (positive for phosphorylated histone H3 (P-H3)) were assayed by flow cytometry 1 hour after IR. The percentage of P-H3 positive cells (unirradiated/irradiated) is plotted for each genotype. Data are representative of at least three independent experiments. (b) The intra S phase checkpoint in hNbs1<sup>657Δ5</sup> (gray triangles), WT (black squares),

Nbs1<sup>Δ/-</sup> (open circles) and Atm<sup>-/-</sup> (open squares) mice as function of IR dose. B cells were stimulated for 48 hours, irradiated with the indicated dose, and thymidine uptake was assessed 4 hrs after IR. Data from triplicate samples are normalized to the counts in un-irradiated controls. Data are representative of at least three independent experiments. (c) Absence of IR induced Mre11 foci in hNbs1<sup>657Δ5</sup> MEFs. Immunostaining of Mre11 (green) and γ-H2AX (red) in MEFs 16 hours after treatment with 10 Gy IR together with the corresponding unirradiated control (0 Gy). DNA was counterstained with DAPI (blue) and images were merged to determine colocalization.

## SUPPLEMENTARY METHODS

**Mice.** Bacteria containing the BAC 255A7 (Research Genetics) were electroporated with mini- $\lambda$  prophage DNA and targeting of the BAC was performed using the two-step recombination method previously described<sup>1</sup>. The targeting was verified by sequencing of the BAC. BACs 255A7 and 255A7-657 $\Delta$ 5 were purified, filtered through a Millipore Biomax-100 unit, and diluted to 0.5–1 ng/ $\mu$ l for pronuclear injection into C57Bl/6 oocytes. The presence of the transgene was determined by screening tail DNA using the following PCR primer pairs: hNBS1F: 5'-GGTCCACCGAACACA TAGACTTACG-3'; hNBS1R 5'- AAGGGAGCCAAAAAGAAAGCAC-3' and hNBS2F 5'- CCCCTTTTGGTGGTCTTACTGAG-3'; hNBS2R 5'- TGACTGGAACCTCTTCTGCTG-3'. Primers hNBS1F /hNBS1R amplify a product of 215 bp, and hNBS2F/ hNBS2R amplify a product of 213 bp at the 3' and 5' ends of hNbs1 respectively. Transgene positive progeny (hNbs1<sup>WT</sup>mNbs1<sup>+/+</sup>) of 4 founder lines were crossed with mNbs1<sup>2</sup> heterozygous mice (mNbs1<sup>+/+</sup>)<sup>5</sup> to produce hNbs1<sup>WT</sup>mNbs1<sup>-/-</sup> mice, in which human Nbs1 substitutes for the endogenous mouse Nbs1. hNbs1<sup>WT</sup>mNbs1<sup>-/-</sup> (abbreviated hNbs1<sup>WT</sup>) mice were born at nearly the expected Mendelian frequency, and were healthy and fertile. Similarly, hNbs1<sup>657 $\Delta$ 5</sup>mNbs1<sup>-/-</sup> and hNbs1<sup>H45A</sup>mNbs1<sup>-/-</sup> mice were generated from intercrosses of mNbs1<sup>+/+</sup> mice<sup>2</sup>.

Nbs1 <sup>$\Delta$</sup>  (CD19cre<sup>+</sup>Nbs1<sup>-loxP</sup>) mice were generated as described<sup>3</sup>. The background of all mice was a mixture between C57Bl/6 and 129Sv strains.

**Histology and meiotic chromosome spreads.** Testes were fixed in buffered 10% formalin and ovaries in Bouin's fixative, and paraffin sections were stained with hematoxylin-eosin. Apoptotic nuclei were detected with TdT-mediated dUTP-biotin nick labeling. Spreads from ovaries of newborn mice were prepared as described previously<sup>4</sup> and immunostained using anti-Scp1 (1:400) and anti-Scp3 (1:800) antibodies as described<sup>5</sup>.

**Chromosome analysis.** Lymph node T cells were stimulated with  $\alpha$ -CD3 and  $\alpha$ -CD28 antibodies for 48 hours as described previously<sup>6</sup> and were arrested at mitosis with Colcemid (Gibco/BRL) treatment at 0.1  $\mu$ g/ml for 0.5–1 h on day 2. Mitotic chromosome spreads were prepared following standard procedures. For FISH analysis, metaphases were hybridized with chromosome 14 specific painting probes and probes specific for the TCR $\alpha$  loci as described<sup>6</sup>. Nested PCR assays for transrearrangements between TCR $\gamma$  and TCR $\beta$  loci were performed as described<sup>7</sup>.

**Intra S phase and G2/M checkpoint assays.** For intra S-phase checkpoints, B

cells were challenged with different doses of  $\gamma$ -irradiation after 48 hrs of stimulation with LPS and IL-4. Cells were immediately pulsed with [<sup>3</sup>H] thymidine (5 $\mu$  Ci) for 4 hours and thymidine uptake was measured. G2/M checkpoint assays were performed on stimulated B cells as described<sup>8</sup>.

**Antibodies for immunofluorescence and Western blotting.** The primary antibodies used for immunofluorescence were: rabbit anti-mNbs1 (1:1000)<sup>9</sup>, anti-hNbs1 (1:1000, Novus Biologicals), anti-Mre11 (1:1000, a gift from J. H. Petrini), anti- $\gamma$ -H2AX (1:1000, Upstate Biotechnology), anti-53BP1 (1:500, Novus Biologicals), anti-PCNA (1:500, Santa Cruz Biotechnology), anti-Nbs1 S343P (1:500, Novus Biologicals) and anti-MDC1 (1:1000)<sup>10</sup>. For Western blotting, primary antibodies were used at the following dilutions: anti-hNbs1 (1:15000; Novus), anti-mNbs1 (1:1000; <sup>9</sup>), anti-Rad50 (1:100; Transduction Laboratories), mouse anti-ATM pS1981 (1:300, Rockland Immunochemicals), mouse anti-ATM (1:500, Novus), rabbit anti-SMC1 pS966 (1:1000, Bethyl Labs), rabbit anti-SMC1 (1:2000, Novus), rabbit anti-p53 pS15 (1:500, Cell Signaling), rabbit anti-p53 (1:1000, Santa Cruz), mouse anti- $\gamma$ -H2AX (1:1000, Upstate Biotechnology), rabbit anti-Chk1 pS345 (1:300, Cell Signaling), mouse anti-Chk2 (1:1500, Upstate Biotechnology), and mouse anti-Actin (1:4000, Sigma).

1. Yang, Y. & Sharan, S. K. A simple two-step, 'hit and fix' method to generate subtle mutations in BACs using short denatured PCR fragments. *Nucleic Acids Res* **31**, e80 (2003).
2. Zhu, J., Petersen, S., Tessarollo, L. & Nussenzweig, A. Targeted disruption of the Nijmegen breakage syndrome gene NBS1 leads to early embryonic lethality in mice. *Curr Biol* **11**, 105–9. (2001).
3. Reina-San-Martin, B., Chen, H. T., Nussenzweig, A. & Nussenzweig, M. C. ATM is required for recombination between immunoglobulin switch regions. *J. Exp. Med.* **200**, 1103–10 (2004).
4. Speed, R. Meiosis in the foetal mouse ovary. I. An analysis at the light microscope level using surface-spreading. *Chromosoma* **85**, 427–437 (1982).
5. Fernandez-Capetillo, O. *et al.* H2AX is required for chromatin remodeling and inactivation of sex chromosomes in male mouse meiosis. *Dev Cell* **4**, 497–508 (2003).
6. Celeste, A. *et al.* Genomic instability in mice lacking histone H2AX. *Science* **296**, 922–7 (2002).
7. Lista, F., Bertness, V., Guidos, C. J., Danska, J. S. & Kirsch, I. R. The absolute number of trans-rearrangements between the TCR $\gamma$  and TCR $\beta$  loci is predictive of lymphoma risk: a severe combined immune deficiency (SCID) murine model. *Cancer Res* **57**, 4408–13 (1997).
8. Fernandez-Capetillo, O. *et al.* DNA damage-induced G2-M checkpoint activation by histone H2AX and 53BP1. *Nat Cell Biol* **4**, 993–7 (2002).
9. Chen, H. T. *et al.* Response to RAG-mediated VDJ cleavage by NBS1 and gamma-H2AX. *Science* **290**, 1962–5. (2000).
10. Lee, A. C., Fernandez-Capetillo, O., Pisupati, V., Jackson, S. P. & Nussenzweig, A. Specific association of mouse MDC1/NFBD1 with NBS1 at sites of DNA-damage. *Cell Cycle* **4**, 177–82 (2005).